Tectonophysics 499 (2011) 118–131

Contents lists available at ScienceDirect

Tectonophysics

journal homepage: www.elsevier.com/locate/tecto

The collision between the Yili and Tarim blocks of the Southwestern Altaids: Geochemical and age constraints of a leucogranite dike crosscutting the HP–LT metamorphic belt in the Chinese Tianshan Orogen

Jun Gao [a,*], Reiner Klemd [b], Qing Qian [a], Xi Zhang [a], Jilei Li [a,b], Tuo Jiang [a], Yongqiang Yang [c]

[a] Key Laboratory of Mineral Resources, Institute of Geology and Geophysics, Chinese Academy of Sciences, P.O. Box 9825, Beijing 100029, China
[b] GeoZentrum Nordbayern, Universität Erlangen, Schlossgarten 5a, 91054 Erlangen, Germany
[c] State Key Laboratory of Geological Processes and Mineral Resources, China University of Geosciences, Beijing 100083, China

ARTICLE INFO

Article history:
Received 2 December 2009
Received in revised form 14 December 2010
Accepted 3 January 2011
Available online 7 January 2011

Keywords:
Leucogranite dike
Collision
Yili block
Tarim block
Tianshan
Southwestern Altaids

ABSTRACT

A *ca.* 600 m-long, 0.5–20 m-wide NW–SE trending granite dike crosscuts the high pressure–low temperature (HP–LT) Tianshan metamorphic belt, the foliation of which is parallel to the main ENE regional trend in the Chinese South Tianshan Orogen. It is mainly composed of plagioclase, K-feldspar, quartz, muscovite, biotite and secondary chlorite, while fluorite, zircon and xenotime occur as accessories. The immediate country rock is a quartz–biotite–plagioclase schist, which grades several tens of meters away from the granite dike into a chlorite–mica–albite schist. The latter schist is intimately intercalated with blueschist layers and boudins. The A/CNK value of the granite dike samples varies from 1.15 to 1.27 indicating a strongly peraluminous composition. CaO/Na_2O ranges from 0.06 to 0.17 and Al_2O_3/TiO_2 from 240 to 525, similar to the ratios of strongly peraluminous (SP) granites exposed in 'high-pressure' collision zones such as the Himalayas. A zircon U–Pb age of 285 Ma was obtained for the granite dike, thus constraining the upper limit for the age of HP–LT metamorphism. The petrological and geochemical data suggest that the SP leucogranite dike intruded during the exhumation of overthickened crust in the post-collisional setting between the Yili (–Central Tianshan) and Tarim blocks. The dataset presented here in conjunction with previously published data corroborate that the HP–LT metamorphism must have occurred earlier than the Permian in the Tianshan Orogen. Therefore, the collision between the Yili (–Central Tianshan) and Tarim blocks and the final amalgamation of the Southwestern Altaids must have been terminated in Late Paleozoic and not in Triassic times as previously suggested.

1. Introduction

The Central Asian Orogenic Belt (CAOB; Zonenshain et al., 1990; Jahn et al., 2000a) or the Altaid Tectonic Collage (Altaids; Sengör et al., 1993) which is sandwiched between the Siberian and Sino-Korean–Tarim–Karakum cratons (Fig. 1a) is the largest Phanerozoic accretionary orogen in the world (Windley et al., 2007; Xiao et al., 2009a, b). Considerable continental growth in the Phanerozoic eon has been advocated for the Altaids as a consequence of lateral accretion of young arc complexes and vertical underplating of mantle derived magmas (Jahn et al., 2000a, b; Gao et al., 2002; Chen and Jahn, 2004; Li et al., 2006; Kröner et al., 2007, 2008). Although arc accretion appears to have been the dominant process in the Altaids, post-collisional mantle-derived magmatic intrusions may also have been involved (Han et al., 1997, 2010; Zhao et al., 2000, 2008; Jahn, 2004; Zhou et al., 2004). The time of the final closure of the Paleo-Asian Ocean and the amalgamation of terranes including oceanic plateaus, oceanic island-arcs, seamounts and Precambrian microcontinents within the Altaids is critical to understanding the mechanism of the Phanerozoic continental growth, which is interpreted as lateral accretion related to oceanic subduction with or without vertical addition of post-collisional mantle-derived magmas (Sengör et al., 1993; Han et al., 1997, 2010; Jahn et al., 2000a, b; Gao et al., 2002; Li et al., 2006; Xiao et al., 2009a, b). The final amalgamation of the southern active margin of the Siberian craton with the passive margin of the Tarim block along the South Tianshan Orogen was proposed to have marked the termination of the Paleo-Asian Ocean in the southwestern corner of the Altaids (Sengör et al., 1993; Xiao et al., 2009a). Therefore, the exact timing of the collision between the Tarim and Yili blocks is decisive for constraining the tectonic evolution and continental growth of the Altaids.

The South Tianshan Orogen, which extends west–east for about 2500 km from Uzbekistan, Tajikistan, Kyrgyzstan, and Kazakhstan to Xinjiang in northwestern China, has traditionally been considered to be a Paleozoic collisional orogen, which had been reactivated during the Cenozoic (Windley et al., 1990; Yin et al., 1998). The collision of the Yili and Tarim blocks is thought to have occurred during the Late Devonian (Xiao et al., 1992; Wang et al., 1994; Xia et al., 2004),

* Corresponding author. Tel.: +86 10 82998245; fax: +86 10 62010846.
E-mail addresses: gaojun@mail.igcas.ac.cn (J. Gao), klemd@geol.uni-erlangen.de (R. Klemd).

0040-1951/$ – see front matter © 2011 Elsevier B.V. All rights reserved.
doi:10.1016/j.tecto.2011.01.001

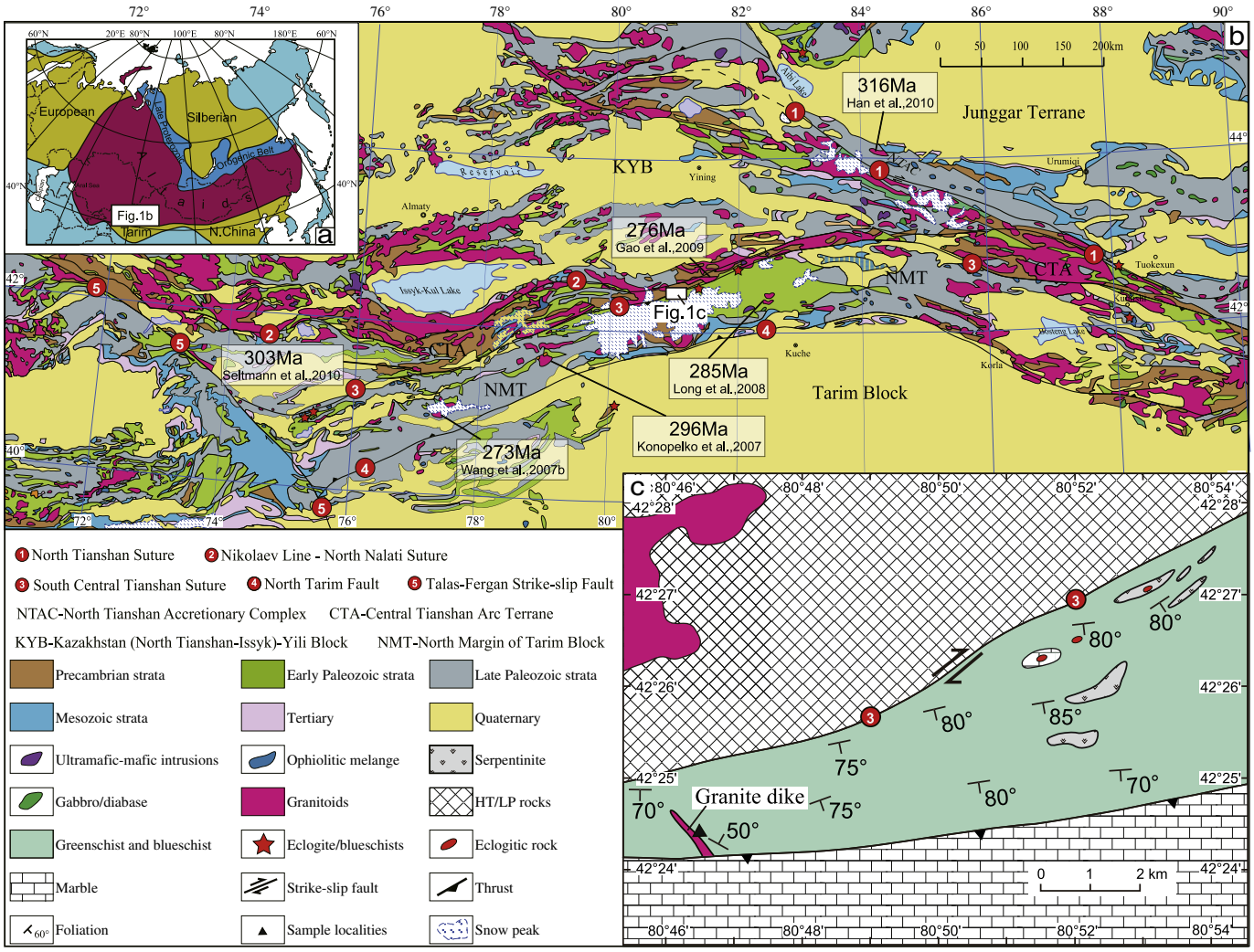

Fig. 1. Tectonic sketch map of the Central Asia Orogenic Belt and the location of the western Tianshan orogen (a; modified after Yakubchuk, 2004), the geological map of the western Tianshan orogen (b; modified after Gao et al., 2009) and the geological map showing the occurrence of a granite dike crosscutting the HP–LT metamorphic belt (c; modified after Liao Ning Institute of Geological Survey, 2005).

Late Devonian–Early Carboniferous (Allen et al., 1992; Charvet et al., 2007; Wang et al., 2010; 2011), Early–middle Carboniferous (Coleman, 1989; Gao et al., 1998; Zhou et al., 2001; Gao and Klemd, 2003; Gao et al., 2009; Su et al., 2010; Biske and Seltmann, 2010), and at the end of Carboniferous to Early Permian (Zonenshain et al., 1990; Chen et al., 1999; Heubeck, 2001; Bazhenov et al., 2003; Xiao et al., 2004, 2006; Klemd et al., 2005; Gao et al., 2006; Li et al., 2006; Solomovich, 2007; Konopelko et al., 2007; Li et al., 2008; Burtman, 2010; Glorie, et al., 2010; Seltmann et al., 2010). A Paleozoic collision has been supported by recent age data from high pressure–low temperature (HP–LT) rocks of the Tianshan Orogen comprising Sm–Nd isochron (omphacite–garnet–glaucophane–whole rock) ages of 343 ± 44 Ma (Gao and Klemd, 2003) and 319 ± 4 Ma (Hegner et al., in press), a $^{40}Ar/^{39}Ar$ crossite age of 344 ± 3 Ma, Rb–Sr isochron ages of 313–302 Ma (mica–whole rocks), $^{40}Ar/^{39}Ar$ phengite ages of 331–310 Ma — (Gao and Klemd, 2003; Klemd et al., 2005; Wang et al., 2010), $^{40}Ar/^{39}Ar$ phengite and glaucophane ages of 327–324 Ma (Simonov et al., 2008) and a U–Pb metamorphic zircon rim age of ca. 320 Ma (Su et al., 2010). However, it was also suggested that the collision for the South Tianshan Orogenic belt in Uzbekistan–Tajikistan–Kyrgyzstan (Brookfield, 2000) and NW China (Zhang et al., 2007a; 2007b; Xiao et al., 2009a) had occurred during the Triassic. The Triassic collision is mainly based on recent SHRIMP U–Pb ages of 233–226 Ma obtained for zircon rims separated from eclogites in NW China (Zhang et al., 2007a). More recently, two HP–LT metamorphic events with Sm–Nd and Lu–Hf garnet ages varying from 308.9 ± 2.0 to 326.8 ± 5.2 Ma and from 243.3 ± 2.9 to 263 ± 10 Ma were proposed for the Tianshan eclogitic rocks (Zhang et al., 2009). Thus, as of yet, no consensus has been reached on the timing of the regional HP–LT metamorphism, which constitutes an excellent collisional marker for an orogeny (Windley, 1995; Liégeois, 1998).

Besides HP–LT rocks, strongly peraluminous (SP) granites are commonly associated with the collision of continental lithosphere (e.g. Le Fort et al., 1987; Nabelek and Bartlett, 1998; Barbarin, 1999). These granites have been suggested to be the result of melting of meta-shales or meta-greywackes during post-collisional processes in various orogens (e.g. Sylvester, 1998). Thus, the presence of SP granites in collisional orogens represents a good hallmark to constrain the collision time of two continents. In this paper we present geochemical and geochronological data of a leucogranite dike which runs across the HP–LT metamorphic belt in the Chinese South Tianshan Orogen and thus constrain the upper age limit for HP–LT metamorphism and subsequent collision between the Tarim and Yili blocks in order to understand the geotectonic framework and the Phanerozoic continental growth of the Altaids.

2. Geological background and sample locality

The Tianshan HP–LT belt extends for 1500 km from Kekesu, Akeyazi and Changawuzi in NW-China, Atabashi of Kyrgyzstan to Fan-Karategin of Tajikistan (Gao et al., 1995; Tagiri et al., 1995; Volkova and Budanov, 1999) along a suture zone between the Yili–Kazakhstan–Kyzylkum and the Tarim–Karakum blocks (Volkova and Budanov, 1999). In the Chinese Tianshan the HP–LT belt extends for at least 200 km along the South Tianshan suture (or South Central Tianshan suture) representing a collisional zone separating the Yili (–Central Tianshan) block to the north and the Tarim block to the south (Fig. 1a). It is mainly composed of blueschist-, eclogite- and greenschist-facies meta-sedimentary rocks and some mafic metavolcanic rocks with N-MORB, E-MORB, OIB and arc basalt affinities (Gao et al., 1999; Gao and Klemd, 2003; Ai et al., 2005; Li et al., 2007; John et al., 2008). Blueschists occur within greenschist-facies metasediments as small discrete bodies, lenses, bands and thick layers. Eclogites are interlayered with the blueschist layers as pods, boudins, thin layers or as massive blocks. Most eclogites have experienced peak metamorphism estimated to range between 480 and 580 °C at 1.4–2.1 GPa at a regional scale (Klemd et al., 2002; Wei et al., 2003; Lin and Enami, 2006). Ultrahigh-pressure peak metamorphic conditions for some eclogites were proposed and controversially discussed (e.g. Zhang et al., 2003a; Klemd, 2003). UHP conditions of 2.7–3.3 GPa at 570–630 °C were reported for metapelitic schists and eclogites from a single locality (Habutengsu valley; Lü et al., 2008, 2009). The peak metamorphic P–T conditions for prograde metapelitic schists vary from 22–23 kbar at 540–550 °C to 32 kbar at 550–570 °C (Wei et al., 2009). Networks of eclogite-facies veins derived from the dehydration of blueschists during prograde and retrograde metamorphism are widely present in the HP–LT metamorphic terrane (Gao and Klemd, 2001; Gao et al., 2007; John et al., 2008; Van der Straaten et al., 2008; Beinlich et al., 2010).

To the north of the HP–LT belt, the Central Tianshan Arc terrane (Fig. 1a) is mainly composed of amphibolite- and granulite-facies rocks, Late Silurian and Early Carboniferous island-arc-type volcanics and volcaniclastic rocks as well as Caledonian–Variscan granitoids (Allen et al., 1992; Gao et al., 1998) and ~430 Ma subduction-related mafic–ultramafic intrusions (Yang and Zhou, 2009) superimposed on a Precambrian basement. In the western segment, north to the Changawuzi valley, low-pressure two-pyroxene granulites with a SHRIMP zircon U–Pb age of 298.5 ± 4.9 Ma were reported and may represent a high temperature–low pressure metamorphic belt related with the HP–LT belts as a paired metamorphic belt (Li and Zhang, 2004). However, a U–Pb zircon age of 1910 Ma had also been derived for the granulite from the same locality (Liao Ning Institute of Geological Survey, 2005). The Central Tianshan Arc terrane is a composite active continental margin the evolution of which was interpreted to be related to the subduction of the 'Terskey Ocean' from the end of Riphean (latest Neo-Proterozoic) until middle Early Ordovician as evidenced by MORB-type basalts with an U–Pb zircon age 516.3 ± 7.4 Ma and adakitic diorites with a U–Pb zircon age of 470 ± 12 Ma (Qian et al., 2009). It amalgamated with the Yili block as a result of the closure of the 'Terskey Ocean' (Gao et al., 2009) and is furthermore related to the subduction of the 'South Tianshan Ocean' from Silurian to latest Carboniferous times as evidenced by U–Pb zircon ages (430 to 330 Ma) of abundant tholeiitic to calc-alkaline I-type granitoids (e.g. Han et al., 2004; Shi et al., 2007; Gao et al., 2009). Inherited zircon grains with $^{206}Pb/^{238}U$ ages between 2478 and 2567 Ma found in Carboniferous magmatic arc-type volcanic rocks indicate that this active margin was superimposed on a Precambrian continental basement (Zhu et al., 2005; Gao et al., 2009).

To the south, the HP–LT belt is overlain by a succession of Paleozoic sedimentary strata, which are considered to represent the passive continental margin of the Tarim block (Allen et al., 1992; Carroll et al., 1995). A few ophiolitic blocks or slices are thrust over the sedimentary sequences as klippen and are possibly crustal remnants of a Silurian–Early Carboniferous ocean between the Tarim- and Yili blocks (Gao et al., 1998). Permian syenites, nepheline syenites, aegirine syenites, two-mica peraluminous granites and A-type rapakivi granites extensively intruded into Paleozoic sedimentary strata (Jiang et al., 1999; Solomovich and Trifonov, 2002; Liu et al., 2004; Konopelko et al., 2007; Solomovich, 2007; Long et al., 2008). Additionally, granites with zircon ages varying from 490 to 386 Ma were also proposed to occur in the eastern segment of the South Tianshan (Hopson et al., 1989; Han et al., 2004; Zhu et al., 2008).

A NW–SE trending and to the NE dipping granite dike with is exposed for a length of *ca.* 600 m and has a width of 0.5 m to 20 m, is rooted in a thrust and runs across the HP–LT metamorphic belt (Fig. 1c and Fig. 2a,b). The dike and its apophyses exhibit a sharp contact with the immediate wall rock (quartz–biotite–plagioclase schist; Fig. 2b,c), the foliation of which dips from NE25°–50° to SE165°–85°. The contact is almost perpendicular to the foliation of the wall rocks (Fig. 2c). The quartz–biotite–plagioclase schist gradually changes over several tens of meters into a greenschist-facies chlorite–mica–albite schist which is intercalated with blueschist layers and boudins (e.g., Gao et al., 1999). About 8 km to the northeast of the dike (Fig. 1c), eclogite boudins have been reported to occur within marbles (Zhang et al., 2003b) and rodingites which were interpreted to have been derived from retrograded eclogite enclosed in serpentinized ultramafic rocks (Li et al., 2007, 2010a, b). The samples used in this study were collected predominantly from the dike and immediate country rocks (Fig. 1c).

3. Petrography of granite dike and country rocks

3.1. Granite dike

The massive granite dike lacks any foliation and mainly consists of coarse-grained plagioclase (~35 vol.%) and K-feldspar (~32 vol.%), quartz (~30 vol.%), muscovite, biotite, secondary chlorite, and accessory fluorite, zircon and xenotime. Muscovite, biotite and fluorite compose less than 3 vol.% indicating a leucogranitic composition according to the definition of Sylvester (1998). Fine-grained muscovite, biotite and fluorite grains either occur as inclusions in plagioclase or as unorientated matrix minerals (Fig. 2d and e). Biotite is partly retrograded to chlorite. Few fine-grained xenotime grains occur as inclusions in fluorite. No micro-deformed structures such as bended mechanical twins of plagioclase or recrystallization features such as sub-grains and undulatory extinction of quartz were observed.

3.2. Country rocks

The immediate country rock of the granite dike is a quartz–biotite–plagioclase schist which mainly comprises plagioclase, quartz and biotite with accessory garnet, andalusite, tourmaline, calcite and titanite/ilmenite. Plagioclase porphyroblasts contain garnet, biotite and tourmaline inclusions (Fig. 2f). Orientated fine-grained biotite defines a foliation. The quartz–biotite–plagioclase schist grades into a chlorite–mica–albite schist, which contains the greenschist-facies mineral assemblage albite, white mica, chlorite, quartz, and accessory rutile, titanite and ilmenite. Albite occurs as porphyroblast in a foliated matrix (Fig. 2g). High pressure minerals or relicts were not found in the immediate country rocks of the granite dike. The intercalated blueschist boudins are exposed within the country greenschists and display the mineral assemblage garnet, glaucophane, clinozoisite, albite, chlorite, rutile and titanite (Fig. 2h). Garnet porphyroblasts contain glaucophane, paragonite and rutile inclusions and are retrograded to chlorite along fractures. Fine-grained glaucophanes which are intimately intergrown with clinozoisite define a foliation parallel to that of the surrounding greenschist-facies schists.

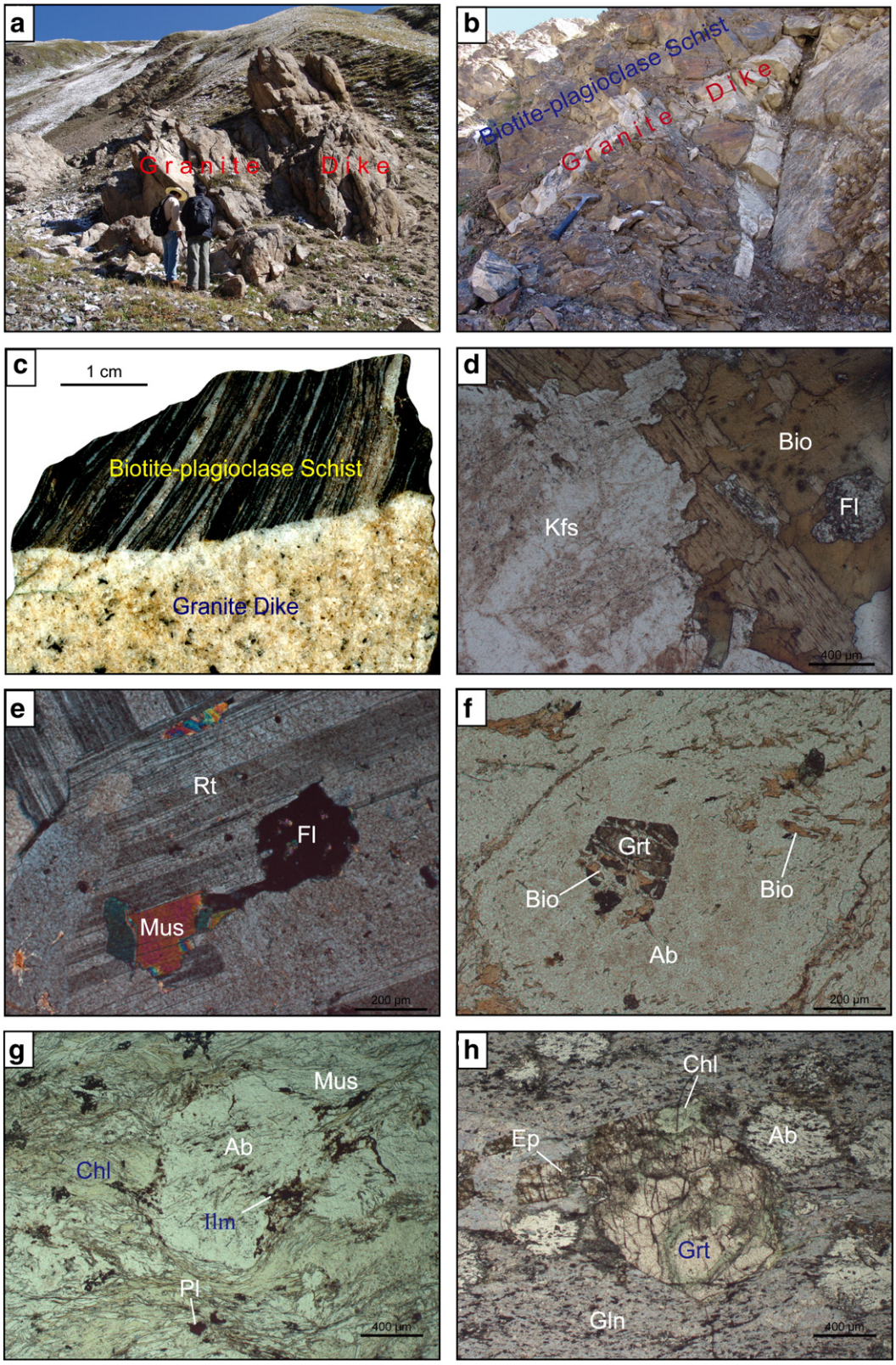

Fig. 2. (a and b) A granite dike exposed in the HP–LT metamorphic belt, (c) the sharp contact between the granite dike and the host biotite–plagioclase schist, (d) K-feldspar, biotite and fluorite in the granite dike (plane-polarized light, sample TGLS8), (e) muscovite and fluorite inclusions in plagioclase of the granite dike (cross-polarized light, sample TGLS8), (f) biotite, garnet and plagioclase in the quartz–biotite–plagioclase schist (plane-polarized light, sample TGLS11), (g) the mineral assemblage muscovite, chlorite, albite, rutile, and ilmenite in the chlorite–mica–albite schist (plane-polarized light, sample TGLS21), and (h) the mineral assemblage garnet, glaucophane, epidote, chlorite and albite inthe blueschist (plane-polarized light, sample ZO88). Kfs — K-feldspar, Bio — biotite, Fl — fluorite, Pl — plagioclase, Mus — muscovite, Grt — garnet, Ab — albite, Chl — chlorite, Rt — rutile, Ilm — ilmenite, Ep — epidote, Gln — glaucophane.

4. Analytical method

The major and minor element compositions of silicate minerals of Sample TGSL11 were performed using a Cameca SX50 electron microprobe at the Institute of Mineralogy of the Universität Würzburg. For other samples (TGSL6, 8, 21 and Z088), analyses were conducted on a JEOL JXA 8100 Superprobe at the Department of Geology, Peking University, in wavelength-dispersive mode, using an accelerating voltage of 15 kV, beam current of 1×10^{-8} A and spot diameter of 1 μm. Matrix corrections were carried out using the PRZ correction program supplied by the manufacturer.

After careful microscopic investigation, 7 representative samples were selected for chemical analysis. They were crushed by a hardened jaw crusher, hand-picked, and then grinded in an agate mill into a powder with a grain size less than 200 mesh (80 μm). Major oxides were obtained by X-ray fluorescence analysis (XRF; PHILIPS PW1480) using fused glass disks at the Institute of Geology and Geophysics, Chinese Academy of Sciences (IGGCAS). Uncertainties for most major oxides are <2%, for MnO and P_2O_5, <5%, and the totals are within 100 ± 1%. Loss on ignition (LOI) was measured after heating the samples to 1000 °C. Trace element concentrations were analyzed by inductively coupled plasma mass spectrometry (ICP-MS; Finnigan Element) at IGGCAS. Relative standard deviations (RSD) are within ± 10% for most trace elements.

Nd isotopic compositions were determined on a Finnigan MAT-262 mass spectrometer operated in static mode at the Isotope Laboratory of IGGCAS. About 100–150 mg of whole rock powder was completely decomposed in a mixture of HF-HClO4. Sr and REE were separated using quartz columns with a 5 ml resin bed of AG 50 W-X12, 200–400 mesh. Nd was separated from other REEs by quartz columns using 1.7 ml Teflon® powder as cation exchange medium. Procedural blanks were <50 pg for Nd. Nd was loaded as phosphates and measured in a Re-double-filament configuration. $^{143}Nd/^{144}Nd$ ratios were normalized to $^{146}Nd/^{144}Nd = 0.7219$.

Zircon grains separated from two samples were prepared using conventional crushing techniques and then hand-picked. They were mounted in epoxy resin disks and polished with 0.25 μm diamond paste. Zircon grains, together with the zircon standards TEMORA, were mounted in epoxy mounts which were then polished to section the crystals in half. All zircon grains were documented with transmitted and reflected light micrographs as well as cathodoluminescence (CL) images to reveal their internal structures. The CL imaging was carried out on a LEO1450VP scanning electron microscope with a MiniCL detector at the Institute of Geology, Chinese Academy of Geological Sciences. Measurements of U, Th and Pb were conducted using the Cameca IMS-1280 ion microprobe at IGGCAS. The O_2^- primary ion beam was accelerated at −13 kV, with an intensity of *ca.* 10 nA. The ellipsoidal spot is 20 × 30 μm in diameter. Positive secondary ions were extracted with a 10 kV potential. Oxygen flooding was used to increase the O_2 pressure to *ca.* 5×10^{-6} Torr in the sample chamber, enhancing Pb^+ sensitivity to a value of ≥25 cps/nA/ppm. U–Th–Pb ratios were determined relative to the TEMORA standard zircon ($^{206}Pb/^{238}U = 0.0668$ corresponding to 417 Ma, Black et al., 2003), and the absolute abundances were calibrated to the 91,500 standard zircon (U = 81.2 ppm and Th = 29 ppm, Wiedenbeck et al., 1995). Analyses of standards were interspersed with those of unknown grains, using operating and data processing procedures similar to those described by Li et al. (2009). The mass resolution used to measure Pb/Pb and Pb/U isotopic ratios was ca. 5400 to separate Pb^+ peaks from isobaric interferences. Measured compositions were corrected for common Pb using non-radiogenic ^{204}Pb. Corrections are sufficiently small to be insensitive to the choice of common Pb composition, and an average of present-day crustal composition (Stacey and Kramers, 1975) is used for the common Pb assuming that the common Pb is largely surface contamination introduced during sample preparation. Uncertainties on individual analyses in data tables are reported at a 1 sigma level; mean ages for pooled U/Pb analyses are quoted with 95% confidence interval. Data reduction was carried out using the Isoplot/Ex v. 3.11 program (Ludwig, 2001). Concordia age values are given at 2 sigma at 95% confidence level.

5. Results

5.1. Mineral chemistry

The representative major element composition of minerals in the granite dike and the immediate country rocks and intercalated blueschist are presented in Table 1.

5.1.1. Granite dike

Biotite has 2.83 Si per formula unit (p.f.u.), 1.65 Fe^{2+} (p.f.u.) and 0.12 Mg (p.f.u.). Muscovite has a Si content in the range of 3.09–3.17 (p.f.u). The plagioclase is albite and the alkaline feldspar is composed of *ca.* 90 mol% orthoclase and 10 mol% albite component. Chlorite grew at the expense of biotite and has a $Fe^{2+}/(Fe^{2+}+Mg)$ value of *ca.* 0.94.

5.1.2. Country rocks

Garnet in the blueschist shows a well-defined major-element prograde growth zoning as indicated by an increase of the pyrope/almandine ratio and a decrease of the spessartine component from core to rim, i.e. a core composition of $Alm_{62}Prp_{3.4}Grs_{30}Sps_{5.1}$ and a rim composition of $Alm_{60}Prp_{4.32}Grs_{34}Sps_{1.39}$. The composition and zoning behavior of the garnet is similar to that reported for garnets from other Tianshan eclogite and blueschist localities (e.g. Gao et al., 1999). Garnet in the quartz–biotite–plagioclase schist is almost homogeneous and has a higher spessartine component (17 mol%) and lower grossular component (19 mol%) when compared with the composition of garnet in the blueschist. Glaucophane in the blueschist has a $Fe^{3+}/(Fe^{3+}+Al^{VI})$ value in the range of 0.10–0.20 and a B_{Na} value varying from 1.88 to 1.97. Clinozoisite has a Ps-content [$100\times Fe3^+/(Fe3^+ + Al)$] of *ca.* 12. Biotite of the quartz–biotite–plagioclase schist has 2.43 Si (p.f.u.), 1.09 Fe^{2+}(p.f.u.) and 0.99 Mg (p.f.u.). The greenschist-facies chlorite–mica–albite schist contains phengite and paragonite. The former has a Si content in the range of 3.37–3.45 (p.f.u.) and the latter 3.04 (p.f.u.). These compositions are similar to those previously reported for white mica in greenschist-facies schists and blueschists from the same area (Changawuzi section, Gao et al., 1999). The plagioclase in both the chlorite–mica–albite schist and blueschist is close to the pure albite end-member. However plagioclase in the quartz–biotite–plagioclase schist has a Ca content of 0.13 p.f.u. and is thus classified as oligoclase. Chlorite in the chlorite–mica–albite schist is usually intergrown with phengite, paragonite and albite and its $Fe^{2+}/(Fe^{2+}+Mg)$ varies from 0.56 to 0.59. Chlorite in the blueschist grew at the expense of garnet and has $Fe^{2+}/(Fe^{2+}+Mg)$ from 0.52 to 0.61. Andalusite in the quartz–biotite–plagioclase schist is almost pure Al_2SiO_5.

5.2. Whole rock chemistry

Major, trace element and Nd isotopic compositions of seven samples from the granite dike are presented in Table 2. The samples have an average SiO_2 content of 77.87 wt.% and are granites *sensu strictu* based on the classification of Middlemost (1994). Al_2O_3 ranges from 11.94 to 13.44 wt.%, Na_2O from 3.58 to 3.95 wt.%, K_2O from 3.04 to 4.00 wt.% and TiO_2 from 0.02 to 0.06 wt.%. CaO/Na_2O ranges from 0.06 to 0.17 and Al_2O_3/TiO_2 from 240 to 525. All samples are strongly peraluminous with an A/CNK value [molar Al2O3/[CaO + Na2O + K2O]] varying from 1.15 to 1.27 (Fig. 3) with an average of 1.21. Their chondrite-normalized rare earth element pattern displays a negative Eu anomaly (Fig. 4a), a slight LREE-depletion and HREE-enrichment. $(La/Yb)_N$ ranges from 0.35 to 0.50, $(Gd/Yb)_N$ from 0.31 to 0.48 and Eu/

Table 1
Representative major element composition of minerals in the granite dike and its country rocks from the Tianshan Orogen in NW China.

Sample	TGSL8	TGSL8	TGSL8	TGSL8	TGSL8	TGSL11	TGSL11	TGSL11	TGSL6	TGSL21	TGSL21	TGSL21	TGSL21	Z088	Z088	Z088	Z088	Z088	Z088	Z088
Location in the granite dike						Immediate country biotite–plagioclase schist country greenschist								Country blueschist						
Mineral	Pl	Kfs	Bio	Mus	Chl	Grt	Bio	Pl	And	Mus	Mus	Pl	Chl	Grt-c	Grt-r	Gln	Gln	Chl	Epi	PL
SiO_2	68.33	64.72	35.43	46.21	23.60	36.76	34.98	64.25	36.06	51.75	47.59	67.74	25.44	37.39	37.49	56.96	56.53	25.48	38.59	68.23
TiO_2	0.00	0.06	1.22	0.00	0.05	0.10	2.02	0.00	0.18	0.16	0.03	0.00	0.07	0.09	0.17	0.08	0.13	0.09	0.11	0.00
Al_2O_3	19.41	18.94	19.97	36.24	21.73	20.76	20.50	22.67	62.23	26.65	39.26	19.83	22.16	21.55	21.83	10.69	11.06	19.64	28.55	19.57
Cr_2O_3	0.00	0.00	0.00	0.05	0.13	0.03	0.06	0.00	0.00	0.05	0.04	0.07	0.10	0.02	0.05	0.05	0.02	0.01	0.04	0.05
FeO	0.00	0.02	24.70	1.06	40.17	26.39	18.72	0.11	0.38	3.13	0.51	0.03	28.97	27.74	27.08	13.44	13.33	32.68	6.13	0.01
Fe_2O_3	0.00	0.00	0.00	0.00	0.00	0.26	0.00	0.00	0.00	0.00	0.00	0.00	0.00	0.00	0.00	0.00	0.00	0.00	0.00	0.00
MnO	0.05	0.00	1.34	0.06	1.33	8.39	0.18	0.00	0.05	0.11	0.00	0.00	0.18	2.26	0.62	0.00	0.01	0.26	0.00	0.02
MgO	0.00	0.00	1.04	0.05	1.36	1.23	9.57	0.00	0.13	3.05	0.18	0.00	12.26	0.86	1.10	8.31	8.37	9.93	0.03	0.01
CaO	0.10	0.04	0.01	0.00	0.09	6.08	0.03	2.71	0.00	0.00	0.14	0.05	0.08	10.39	12.24	0.67	0.66	0.08	24.23	0.07
Na_2O	11.78	1.14	0.16	0.16	0.09	0.00	0.24	9.86	0.00	0.23	6.06	11.57	0.09	0.02	0.00	6.94	7.22	0.17	0.00	11.57
K_2O	0.09	15.82	9.30	10.77	0.01	0.00	8.56	0.21	0.00	10.24	1.26	0.04	0.06	0.00	0.00	0.00	0.01	0.01	0.00	0.08
Total	99.76	100.74	93.17	94.60	88.56	100.00	94.86	99.81	99.03	95.37	95.07	99.33	89.41	100.32	100.58	97.14	97.34	88.35	97.68	99.61
Si	2.99	2.97	2.84	3.09	2.69	2.97	2.43	2.83	0.99	3.45	3.04	2.98	2.68	2.98	2.96	7.95	7.85	2.78	3.00	2.99
Ti	0.00	0.00	0.07	0.00	0.00	0.01	0.11	0.00	0.00	0.01	0.00	0.00	0.01	0.01	0.01	0.01	0.01	0.01	0.01	0.00
Al	1.00	1.02	1.88	2.85	2.92	2.01	1.68	1.18	2.00	2.09	2.95	1.03	2.74	2.02	2.04	1.76	1.81	2.52	2.61	1.01
Cr	0.00	0.00	0.00	0.00	0.01	0.00	0.00	0.00	0.00	0.00	0.00	0.00	0.01	0.00	0.00	0.01	0.00	0.00	0.00	0.00
Fe^{3+}	0.00	0.00	0.00	0.00	0.00	0.00	0.00	0.00	0.00	0.00	0.00	0.00	0.00	0.00	0.00	0.20	0.40	0.00	0.36	0.00
Fe^{2+}	0.00	0.00	1.65	0.06	3.83	1.82	1.09	0.00	0.01	0.18	0.03	0.00	2.55	1.85	1.79	1.37	1.15	2.98	0.00	0.00
Mn	0.00	0.00	0.09	0.00	0.13	0.50	0.01	0.00	0.00	0.01	0.00	0.00	0.02	0.15	0.04	0.00	0.00	0.02	0.00	0.00
Mg	0.00	0.00	0.12	0.01	0.23	0.12	0.99	0.00	0.01	0.30	0.02	0.00	1.92	0.10	0.13	1.73	1.73	1.61	0.00	0.00
Ca	0.01	0.00	0.00	0.00	0.01	0.57	0.00	0.13	0.00	0.00	0.01	0.00	0.01	0.89	1.04	0.10	0.10	0.01	2.02	0.00
Na	1.00	0.10	0.03	0.02	0.02	0.00	0.03	0.84	0.00	0.03	0.75	0.99	0.02	0.00	0.00	1.88	1.94	0.04	0.00	0.98
K	0.01	0.93	0.95	0.92	0.00	0.00	0.77	0.01	0.00	0.87	0.10	0.00	0.01	0.00	0.00	0.00	0.00	0.00	0.00	0.00
Cation	5.00	5.03	7.63	6.95	9.85	8.00	7.10	5.00	3.01	6.94	6.90	5.00	9.95	8.00	8.01	15.00	15.00	9.97	8.00	4.99
O	8	8	11	11	14.00	12	11	8	5	11	11	8	14	12	12	23	23	14	12.5	8
Alm						60.44								61.78	59.71					
Gro						18.85								29.57	34.42					
Pyr						3.97								3.41	4.32					
Spe						16.68								5.10	1.39					

Pl—plagioclase, Kfs—K feldspar, Bio—biotite, Mus—muscovite, Chl—chlorite, Grt—garnet, And—andalusite, Gln—glaucophane, Epi—Epidote, Alm—almandine, Gro—grossular, Pyr—pyrope, Spe—spessartine.
c—the core of mineral, r—the rim of mineral.

Table 2
Major, trace element and Nd isotopic compositions of the granite dike from the Tianshan Orogen in NW China.

Sample	TGLS1	TGLS5	TGLS7	TGLS8	TGLS9	LGLS14	TGLS18
SiO_2	77.63	78.34	80.11	77.28	76.72	76.83	78.18
TiO_2	0.05	0.05	0.02	0.06	0.04	0.05	0.04
Al_2O_3	13.31	13.43	11.94	13.23	13.44	13.41	13.05
Fe_2O_3T	0.82	0.31	0.34	0.85	0.79	0.92	0.47
MnO	0.01	0.02	0.01	0.03	0.03	0.04	0.01
MgO	0.15	0.18	0.12	0.08	0.06	0.07	0.11
CaO	0.51	0.43	0.23	0.65	0.63	0.53	0.53
Na_2O	3.58	3.95	3.64	3.76	3.77	3.68	3.59
K_2O	3.40	3.04	3.39	3.67	3.98	4.00	3.59
P_2O_5	0.01	0.03	0.01	0.01	0.01	0.01	0.01
LOI	0.52	0.50	0.28	0.58	0.58	0.44	0.52
Total	100.00	100.27	100.09	100.20	100.04	99.98	100.09
A/CNK	1.27	1.27	1.18	1.17	1.15	1.18	1.22
CaO/Na2O	0.14	0.11	0.06	0.17	0.17	0.14	0.15
Al_2O_3/TiO_2	252	298	525	240	318	250	307
Be	11.4	7.91	3.65	7.66	7.03	9.46	6.33
Sc	1.96	1.06	1.51	1.97	1.60	1.57	1.92
V	0.417	2.28	0.538	1.15	0.373	1.16	0.679
Cr	0.150	1.85	1.79	0.980	0.478	0.205	2.08
Co	0.339	0.354	0.157	0.280	0.226	0.249	0.357
Ni	0.644	1.71	1.30	0.820	14.7	0.606	1.18
Ga	21.8	16.4	23.2	22.7	24.5	23.8	19.1
Rb	318	352	586	561	606	646	295
Sr	22.7	33.6	19.3	24.1	25.6	22.9	22.9
Cs	10.9	9.42	13.3	18.1	14.2	28.5	7.96
Ba	90.1	122	70.4	40.2	34.2	40.7	75.7
Y	117	50.4	33.7	105	137	115	68.4
Nb	37.7	24.1	51.5	25.6	30.0	36.1	39.3
Ta	11.3	7.92	29.89	6.35	7.35	8.69	7.96
Zr	103	105	37.6	87.6	86.1	83.8	104
Hf	7.24	6.90	4.77	5.51	6.02	5.52	7.01
Pb	43.3	56.0	57.4	52.0	54.0	59.7	67.3
Th	33.1	31.5	13.3	27.6	31.2	32.7	30.6
U	19.8	16.3	19.0	11.6	15.1	14.5	18.3
La	10.3	5.19	5.30	10.4	9.49	12.2	6.46
Ce	25.6	11.6	13.0	25.4	23.8	30.4	14.0
Pr	3.65	1.30	1.73	3.53	3.48	4.14	1.75
Nd	15.6	7.38	8.44	16.4	15.5	17.6	6.83
Sm	6.10	2.46	3.45	6.35	6.95	6.76	2.71
Eu	0.115	0.180	0.044	0.093	0.074	0.089	0.094
Gd	8.43	3.86	4.21	8.31	8.70	8.39	4.23
Tb	2.15	0.985	1.22	1.97	2.26	2.13	1.15
Dy	17.1	7.94	9.41	15.6	18.3	17.2	9.78
Ho	4.22	1.92	2.25	3.70	4.44	4.21	2.53
Er	13.9	6.07	7.59	11.9	14.2	13.2	8.43
Tm	2.39	1.03	1.39	2.04	2.43	2.44	1.50
Yb	16.6	7.12	10.3	14.1	18.2	17.2	11.3
Lu	2.78	1.16	1.68	2.26	2.95	2.57	1.87
∑REE	129	58.2	70.0	122	131	139	72.6
Eu/Eu*	0.049	0.178	0.035	0.039	0.029	0.036	0.085
(La/Yb)N	0.419	0.493	0.348	0.499	0.353	0.482	0.388
$^{147}Sm/^{144}Nd$		0.2017	0.2468	0.2342	0.2705		
$^{143}Nd/^{144}Nd$		0.512478	0.512556	0.512570	0.512611		
2σ error		0.000010	0.000012	0.000012	0.000013		
εNd (285 Ma)		−3.31	−3.42	−2.69	−3.21		

Total iron as Fe_2O_3; A/CNK = molar ratio of Al2O3/(CaO + Na2O + K2O).

Eu* from 0.036 to 0.178. The pattern also displays negative anomalies for Ba, Sr, Ti and Ce and positive anomalies for Cs, Rb and Pb in a primitive mantle (PM)-normalized spidergram (Fig. 4b). The Sr concentration varies between 19.3 and 33.6 ppm with an average of 24.2 ppm similar to that of the primitive mantle (21.1 ppm, Sun and McDonough, 1989). Furthermore, the $\varepsilon Nd_{(285Ma)}$ of −2.69 to −3.42 is higher than that of typical continental crust (White, 2007).

5.3. U–Pb age dating of zircon

U–Pb ages of zircon grains from sample TGLS8 were obtained with a Cameca Ion microprobe. The results are presented in Table 3. Zircon grains show a sharp euhedral habit (equant, stubby or prismatic; Fig. 5a to j) and range in size from 60 to 200 μm with a ratio of length to width from 1:1 to 3:1. They are colorless to light pink, transparent and euhedral with well-developed concentric oscillatory zoning, indicating a magmatic origin. They were divided into two groups according to the cathodoluminescence image. The first group displays a core and rim texture, both of which are oscillatory. The core of some zircon grains (Fig. 5a to c) is relatively darker than the rim, whereas the core of others (Fig. 5d) is relatively lighter than the rim. The darker domain has a relatively higher uranium content compared with the lighter domain. For example, the uranium content of the darker rim (Fig. 5d) is 1593 ppm and that of the lighter core is 200 ppm (Table 3). The second group (Fig. 5e to j) displays well-developed concentric oscillatory zoning only.

18 analyzed spots record $^{206}Pb/^{238}U$ concordant ages ranging from 280.0 ± 4.3 Ma to 290.5 ± 4.3 Ma, with a concordia age of 284.9 ± 2.0 Ma as 2 sigma percent and MSWD (of concordance) = 0.28, and a weighted mean $^{206}Pb/^{238}U$ age of 284.8 ± 2.0 Ma (MSWD = 0.38)

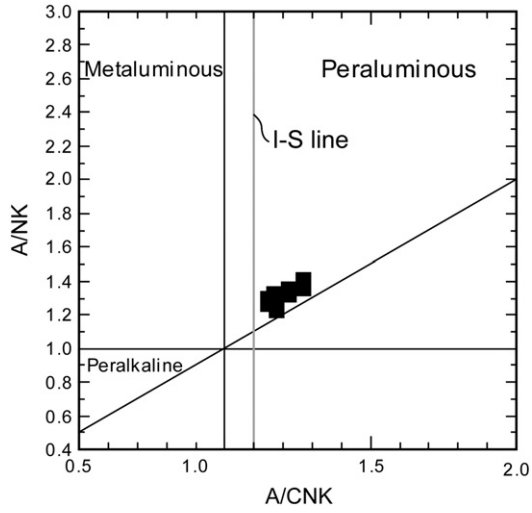

Fig. 3. A/CNK *versus* A/NK diagram of granites (Shand's molar parameters in the diagram after Maniar and Piccoli, 1989).

(Fig. 5k and l). The Th/U ratio of the measured spots varies from 0.210 to 0.601. The darker core of a zircon (Fig. 5b) of the first group has a $^{206}Pb/^{238}U$ age of 282.7 ± 4.4 Ma (Table 3), overlapping within error with the concordia age and the weighted mean age. Furthermore, the core of one zircon grain from the first group has – within error – the same $^{206}Pb/^{238}U$ age as its rim (287.5 ± 4.3 Ma *versus* 286.7 ± 4.4 Ma; Table 3; Fig. 5d).

6. Discussion

6.1. Tectonic setting and origin of the granite dike

SP granitoids are commonly produced by melting of crustal rocks during post-collisional orogenic processes as a result of the exhumation of overthickened crust (e.g. Sylvester, 1998; Barbarin, 1999). For example, in the Himalayas, the collision of India and Asia took place at *ca.* 55 Ma (Yin and Harrison, 2000; Wu et al., 2008) and SP leucogranites intruded between 24 and 14 Ma in the High Himalayas (Le Fort et al., 1987; Schärer et al., 1986; Searle et al., 1997) and between 27.5 and 10 Ma in the North Himalaya (Zhang et al., 2004); in the European Alps, the HP metamorphic event was dated at *ca.* 45 Ma (e.g. Rubatto and Hermann, 2003) and SP granites formed between 32 and 30 Ma (e.g. von Blanckenburg, 1992; Bellieni et al., 1996). The granite dike in this study has a mineral assemblage and bulk chemistry (see above) which are similar to those of strongly peraluminous granitoids related to continental collision events (e.g. Barbarin, 1996, 1999). It probably runs along a NW transcurrent fracture and is rooted by a thrust fault (Fig. 1c), indicating that its tectonic setting is also in agreement with that of peraluminous granitoids which usually occur along major shear and thrust zones crosscutting thickened continental crust (Barbarin, 1999).

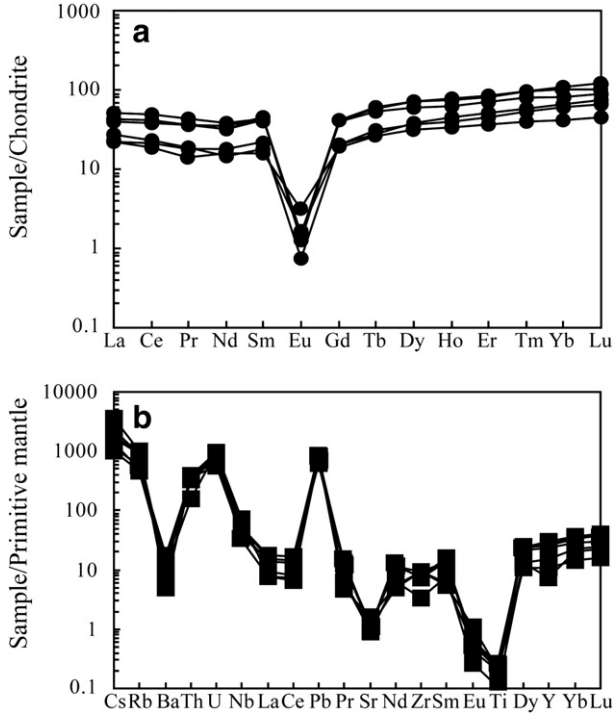

Fig. 4. Chondrite-normalized REE diagrams (a; normalization values are after Taylor and McLennan, 1985) and primitive mantle-normalized spidergrams (b; normalization values are after Sun and McDonough, 1989) of granites.

However, the Al_2O_3 content (11.94 to 13.44 wt.%) is somewhat lower (13.2 to 15.7 wt.%) and the SiO_2 content (76.7 to 80.3 wt.%) somewhat higher (71 to 75.7 wt.%) than that of the SP leucogranites in the High and North Himalayas (Le Fort et al., 1987; Inger and Harris, 1993; Searle et al., 1997; Zhang et al., 2004). Furthermore, CaO/Na_2O (0.06–0.17) and Al_2O_3/TiO_2 (240–525) are similar to those of post-collisional SP granites which have been suggested to have formed by melting of pelites in 'high-pressure' collision zones such as the Himalaya and the European Alps (e.g. Sylvester, 1998). The negative Ba, Sr, Ti and positive Cs, Rb, Pb anomalies in the primitive mantle-normalized spidergram (Fig. 4b) are also similar to the trace element pattern of leucogranites (Guo and Li, 2007). All samples plot in the withinplate field of tectonic discrimination diagrams such as Y + Nb *versus* Rb and Y *versus* Nb (Pearce et al., 1984) — (Fig. 6). In the Rb/Ba–Rb/Sr diagram for SP granite intrusions (Sylvester, 1998; Dahlquist et al., 2007), all samples plot in the low CaO/Na_2O and clay-rich source field (Fig. 7). Three of the samples plot in the field of Himalaya SP leucogranites, while the others plot just above it due to their low Sr and Ba concentrations (average 24.2 ppm and 67.6 ppm, respectively). Additionally, when compared with the SP leucogranites in the High and North Himalayas (Inger and Harris, 1993; Zhang et al., 2004), the granite dike has relatively higher εNd (285 Ma) values from −2.69 to −3.42 indicating some contamination by mantle-derived magmas. Consequently, the petrographic and geochemical features favour a post-collisional 'high-pressure' collision setting for the granite dike which crosscuts the high-pressure/low-temperature metamorphic belt in the Chinese Tianshan. Geochemically similar Permian two-mica peraluminous leucogranites in the Kyrgyz South Tianshan were also interpreted to have formed subsequent to the collision of the Tarim and Kazakh (Yili) blocks (Solomovich, 2007).

6.2. Constraints on the collision between the Yili (–Central Tianshan) and Tarim blocks

As mentioned above, the various geochronological data obtained for the Tianshan high-pressure/low-temperature metamorphic rocks (e.g. Gao and Klemd, 2003; Klemd et al., 2005; Zhang et al., 2007a, b, 2009) have caused discussions concerning the timing of the collision of the Yili (–Central Tianshan) and Tarim blocks and the final amalgamation of the Southwestern Altaids: late Paleozoic (e.g. Windley et al., 1990; Charvet et al., 2007; Wang et al., 2007a; Gao et al., 2009) *versus* Triassic times (e.g. Zhang et al., 2007a,b; Xiao et al., 2009a). In this study, we provide robust geological and geochronological evidence to constrain the upper limit of the Tianshan HP–LT peak metamorphic age and thus the collisional time of the South Tianshan Orogen. The petrography and mineral chemistry of the SP granite dike and its country rocks demonstrate their crosscutting relationship (Fig. 2b and c). The garnet, biotite, tourmaline and andalusite of the immediate country rocks are typical index minerals

Table 3
SIMS zircon U–Pb data for the granite dike from the Tianshan Orogen in NW China.

Sample/spot	U (ppm)	Th (ppm)	Th/U	f_{206} (%)	$^{207}Pb/^{235}U$	±1σ (%)	$^{206}Pb/^{238}U$	±1σ (%)	$^{207}Pb/^{235}U$ Age (Ma)	±1σρ	$^{206}Pb/^{238}U$ Age (Ma)	±1σ
TGLS8.1	391	109	0.280	0.01	0.32654	2.70	0.0446	1.58	286.9	6.8	281.4	4.3
TGLS8.10	754	274	0.364	0.02	0.32618	1.79	0.0461	1.51	286.6	4.5	290.5	4.3
TGLS8.11	200	67	0.333	0.07	0.32206	2.27	0.0456	1.54	283.5	5.6	287.5	4.3
TGLS8.12	1593	414	0.260	0.01	0.32609	1.66	0.0455	1.56	286.6	4.2	286.7	4.4
TGLS8.14	1272	330	0.259	0.01	0.32581	1.75	0.0457	1.51	286.4	4.4	287.9	4.3
TGLS8.15	629	198	0.315	0.00	0.32674	1.75	0.0449	1.51	287.1	4.4	283.0	4.2
TGLS8.16	202	91	0.451	0.06	0.31740	2.26	0.0447	1.50	279.9	5.5	282.1	4.1
TGLS8.17	177	57	0.324	0.00	0.32015	2.43	0.0444	1.56	282.0	6.0	280.0	4.3
TGLS8.18	416	138	0.332	0.04	0.32585	1.87	0.0454	1.50	286.4	4.7	286.3	4.2
TGLS8.19	315	97	0.307	0.48	0.32700	2.52	0.0448	1.60	287.3	6.3	282.7	4.4
TGLS8.2	388	121	0.311	0.09	0.32072	2.01	0.0450	1.51	282.5	5.0	283.8	4.2
TGLS8.21	118	37	0.314	0.00	0.33005	2.55	0.0453	1.60	289.6	6.5	285.6	4.5
TGLS8.3	316	190	0.601	0.00	0.31948	2.02	0.0454	1.53	281.5	5.0	286.4	4.3
TGLS8.4	664	198	0.298	0.09	0.32405	1.80	0.0452	1.51	285.0	4.5	284.9	4.2
TGLS8.5	856	180	0.210	0.53	0.32633	1.99	0.0454	1.62	286.8	5.0	286.0	4.5
TGLS8.6	203	78	0.387	0.04	0.32715	2.21	0.0451	1.52	287.4	5.6	284.5	4.2
TGLS8.7	631	176	0.279	0.01	0.32967	1.76	0.0453	1.51	289.3	4.4	285.7	4.2
TGLS8.8	209	71	0.340	0.11	0.32320	2.33	0.0447	1.57	284.4	5.8	282.2	4.3

of contact metamorphism (Fig. 2f). The country greenschist-facies rocks which contain blueschist boudins have been interpreted to have undergone a similar high pressure metamorphic evolution history as the blueschists and eclogites (e.g. Klemd et al., 2002; Gao and Klemd, 2003; Zhang et al., 2007a, b). Therefore, even if the dike does not directly cut across the blueschists or eclogites, its intrusion time must be later than the age of the regional retrograded greenschist-facies metamorphism and undoubtedly later than the time of peak HP metamorphism. The Si content of 3.37–3.45 (p.f.u.) obtained for phengite of the greenschist-facies rocks here and the glaucophane relics observed in albite of the greenschist-facies rocks in a former study (Gao et al., 1999) further support this interpretation. The U–Pb concordia age of 284.9 ± 2.0 Ma and a weighted mean $^{206}Pb/^{238}U$ age of 284.8 ± 2.0 Ma, the magmatic concentric oscillatory zoning and the Th/U ratio (0.210 to 0.601) of the zircon grains suggest that the SP leucogranite dike must have formed at *ca.* 285 Ma. The darker core of one zircon grain (Fig. 5b) has a $^{206}Pb/^{238}U$ age of 282.7 ± 4.4 Ma (Table 3), thus overlapping within error with the concordia age and the weighted mean age. In addition the core of another zircon grain has – within error – the same $^{206}Pb/^{238}U$ age as its rim (287.5 ± 4.3 Ma *versus* 286.7 ± 4.4 Ma; Table 3; Fig. 5d). These data preclude the occurrence of inherited zircon cores with much older protolith ages which were reported to occur in the two-mica granites in the Himalaya (Lee and Whitehouse, 2007). Furthermore, the western Tianshan HP belt is generally regarded as an 'Alpine-type' subduction complex, the constituents of which were subducted and exhumed together (e.g. Klemd et al., 2002; Gao and Klemd, 2003; Zhang et al., 2007a, b). Thus the mélange was formed in an accretionary wedge before subduction, eliminating that the SP granite dike is an exotic block which may have intruded into the mélange after the exhumation of greenschists and blueschists. The sharp contact between the dike and immediate country rocks (Fig. 2b,c) and the contact metamorphic index minerals preserved in immediate country rocks (andalusite, tourmaline and garnet, Fig. 2f) strongly supports an intrusive relationship between the granite dike and the country rocks. Thus, the HP–LT metamorphism must have occurred before 285 Ma.

The younger U–Pb zircon ages of 233–226 Ma (Zhang et al., 2007a) and 263–243 Ma (Zhang et al., 2009) were interpreted to be due to the fluid-mediated recrystallization of the zircon grains (e.g., Jong et al., 2009; Su et al., 2010) or the rejuvenation of old mountain belts by intra-continental deformation (e.g., Gilotti and McClelland, 2007), which is supported by the absence of eclogite-facies minerals such as omphacite and phengite in the rim domain of these zircon grains (Zhang et al., 2007a). Furthermore, the Rb–Sr isochron age of 267 ± 5 Ma (Tagiri et al., 1995) is controversial since a Sm–Nd isochron age of 319 Ma was obtained for an eclogite from the same locality (Hegner et al., in press) and in addition, the Upper Permian eclogitic pebble-bearing molasse is exposed unconformably on the eclogite-bearing complex (Tagiri et al., 1995). The SHRIMP zircon weighted mean $^{206}Pb/^{238}U$ age of 291 ± 15 Ma obtained for the rodingites, which are greenschist-facies retrograde products of former eclogites (Li et al., 2010b), further indicate that the peak eclogite facies metamorphism must have occurred before the Permian. Whereas, U–Pb zircon ages of 319.5 ± 2.9 and 318.7 ± 3.3 Ma derived for the metamorphic rim domain which contains omphacite, phengite and rutile inclusions (Su et al., 2010), an U–Pb age of 318 ± 7 Ma for eclogitic rutile (Li et al., 2010a) and a Lu–Hf isochron age of 327 Ma (omphacite–garnet–whole rock; Zhang et al., 2009) of eclogites from the Chinese Tianshan and Sm–Nd isochron (omphacite–garnet–glaucophane–whole rock) ages of 319 Ma of eclogites from the Kyrgyz South Tianshan (Hegner et al., in press) suggest an age of *ca.* 320 Ma for the peak of HP–LT metamorphism. Regarding the relatively older ages such as the Sm–Nd age of 343 ± 44 for eclogites, the $^{40}Ar/^{39}Ar$ age of 344 Ma for crossite and the $^{40}Ar/^{39}Ar$ age of 331–323 Ma for phengite (Gao and Klemd, 2003; Wang et al., 2010), two explanations exist for this age discrepancy: The first explanation involves an isotopic disequilibrium between omphacite and other eclogite-facies mineral phases during HP–LT metamorphism which would explain the Sm–Nd age with a large error (e.g. Schmädicke et al., 1995). The second explanation implies that the occurrence of excess argon reported for phengite and sodic-amphibole from other high-/ultrahigh-pressure metamorphic rocks (e.g., Li et al., 1994) could be a reason for an older (344–323 Ma) $^{40}Ar/^{39}Ar$ plateau age for crossite and phengite. Therefore, the best currently available constraint to the HP metamorphism is ca. 320 Ma, rather than the age of 345 Ma which has been employed as evidence for a Late Devonian to Early Carboniferous collision between the Tarim and Yili blocks (Gao and Klemd, 2003; Charvet et al., 2007; Wang et al., 2010).

Two distinct models have been proposed for the Paleozoic tectonics of the Western Tianshan Orogen (e.g., Windley et al., 1990; Allen et al., 1992; Charvet et al., 2007). One model interpreted the southern margin of the Yili (–Central Tianshan) block as a composite active continental margin, the evolution of which was related to the subduction of both the 'Terskey Ocean' from Cambrian to Middle Ordovician (e.g., Qian et al., 2009 and references herein) and the 'South Tianshan Ocean' from Silurian to latest Carboniferous times as evidenced by U–Pb zircon ages of between 470 and 330 Ma of

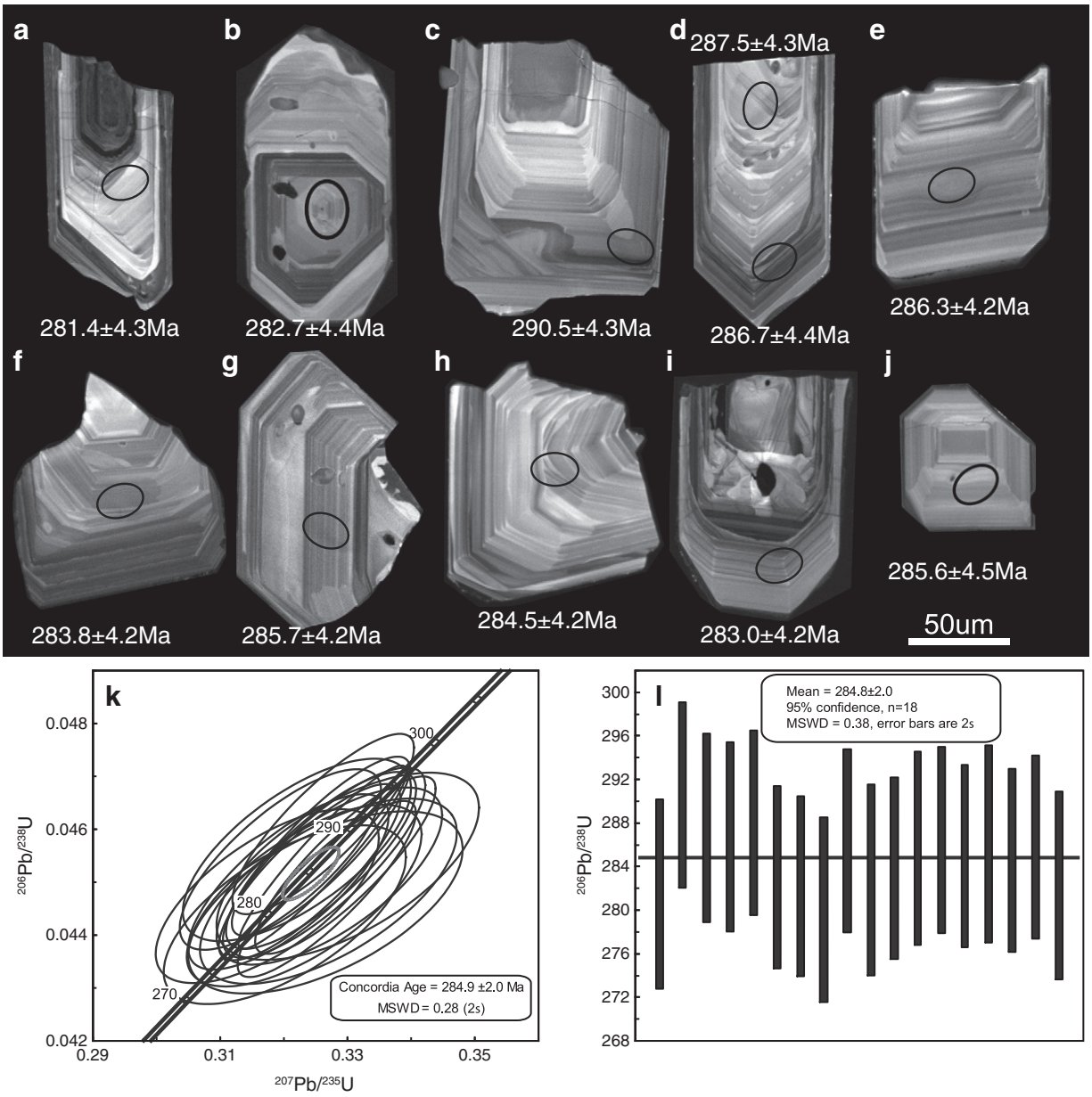

Fig. 5. Representative cathodoluminescence images of zircon grains (a–j), $^{207}Pb/^{235}U$–$^{206}Pb/^{238}U$ concordia diagram (k) and weighted average diagram (l) of the granite dike (sample TGLS8) from Chinese Tianshan.

abundant tholeiitic to calc-alkaline I-type granitoids (e.g., Gao et al. 2009 and references herein). The 'Terskey Ocean' was closed and the Yili and Central Tianshan blocks were amalgamated at the end of middle Ordovician (Qian et al., 2009; Gao et al., 2009). The 'South Tianshan Ocean', which separated the Tarim block to the south and the Yili (–Central Tianshan) block to the north in the late Paleozoic, was suggested to have been subducted to the north according to the island-arc magmatic rocks exposed along the southern margin of the Yili (–Central Tianshan) block (Windley et al., 1990; Allen et al., 1992; Gao and Klemd, 2003; Zhang et al., 2007a). However, another model favors a southern subduction direction for the 'South Tianshan Ocean' as evidenced by a top-to-north ductile shearing foliation preserved in the Central Tianshan and the South Tianshan (e.g. Charvet et al., 2007; Lin et al., 2009; Wang et al., 2010, 2011). A general geodynamic model concerning the subduction direction is beyond the scope of this paper. Here, only the collisional timing between the Yili (–Central Tianshan) and Tarim blocks is discussed on the basis of the geochemical and geochronological datasets of a leucogranite dike crosscutting the HP–LT metamorphic belt in conjunction with the recent published age data obtained for the HP–LT metamorphic rocks and granites and other geological evidence.

The HP–LT metamorphism age of 320 Ma suggests that the initial collision started at the beginning of Late Carboniferous times. The Rb–Sr isochron age (white mica and whole rocks) of 310–302 Ma, which was interpreted to date an incipient greenschist-facies overprint during the exhumation (Klemd et al., 2005), indicates that the HP–LT rocks were exhumed to upper greenschist-facies levels during the collision process of the Tarim and Yili blocks at *ca.* 300 Ma. The break-off of oceanic crust and the exhumation of overthickened crust may have been accompanied by large-scale thrusting and transcurrent shearing (e.g., Barbarin, 1999). Small volumes of SP granite melts with relatively high Al_2O_3/TiO_2 (240–525) and low CaO/Na_2O (0.06–0.17) were generated by anatexis of clay-rich, plagioclase-poor pelitic source rocks (e.g., Sylvester, 1998) and emplaced along the transcurrent shear and thrust zones that crosscut the HP–LT metamorphic belt at *ca.* 285 Ma. The SP leucogranite dike here described shares many similarities with the muscovite-bearing prealuminous granitoids which are associated with crustal thickening resulting

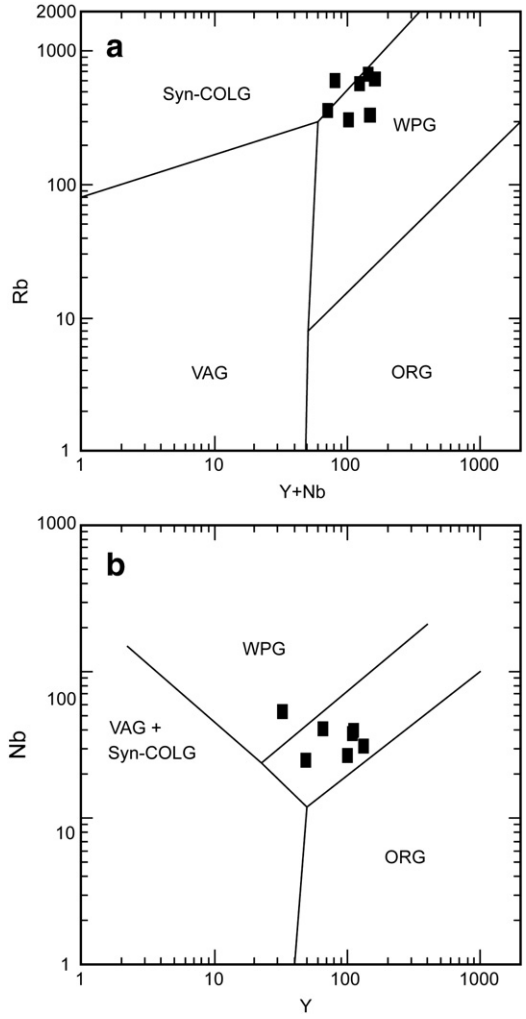

Fig. 6. Tectonic discrimination diagrams for the granite dike from the Chinese Tianshan (Pearce et al., 1984). Y + Nb *versus* Rb (a) and Y *versus* Nb (b).

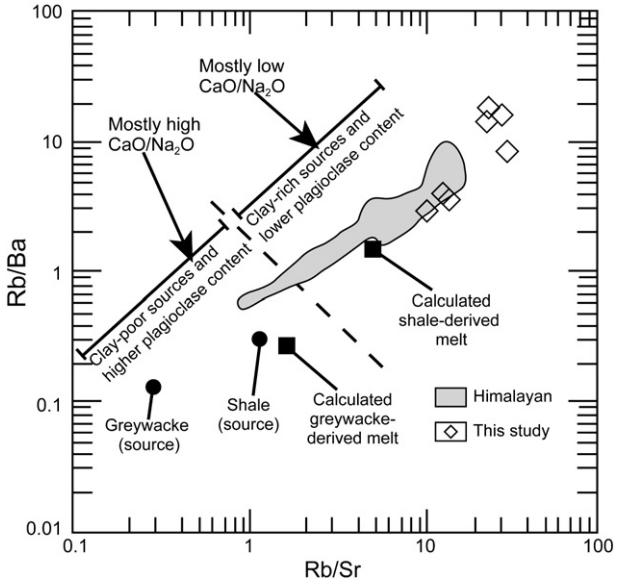

Fig. 7. Rb/Sr *versus* Rb/Ba diagram for strongly peraluminous granitoids modified from Sylvester (1998) and Dahlquist et al. (2007). The dark fields, discontinuous line, and calculated melt are from Fig. 7 of Sylvester (1998).

from the convergence of two continents (Barbarin, 1996). The NW–SE trending SP leucogranite dike runs along a transcurrent fault which crosscuts the foliation of country rocks and the main ENE regional trend (Fig. 1c). Some mantle material may have contaminated the source melting regions of SP leucogranites as is indicated by the εNd (285 Ma) value (from −2.69 to −3.42). However, the upwelling asthenosphere beneath the delaminated lithosphere boundary was largely unable to reach depths sufficiently shallow for melting on a large scale since post-collisional alkaline-granites and cal-alkaline granites are rarely found in the South Tianshan orogen (e.g. Solomovich, 2007; Konopelko et al., 2007; Wang et al., 2007b; Long et al., 2008). The U–Pb age obtained for 494 detrital zircon grains from the eastward-flowing Tekes River and its southern branches flowing through the northern slope of the Chinese South Tianshan varies from 2590 to 268 Ma, with a peak of Paleozoic, however no Mesozoic and Cenozoic zircon grains have been detected (Ren et al., 2010). This further excludes the possibility of a Triassic collision for the Tianshan.

In addition to the above described evidence comprising age data for HP–LT metamorphic rocks, granitoids, granite dike and detrital zircon grains gained from modern river sands in the South Tianshan, further paleomagnetic and geological data also imply that the Western Tianshan Orogen was formed in Late Paleozoic, and not in Triassic times. Further supporting evidence includes: (1) the paleomagnetic data indicate that the North Tianshan (Kazakhstan–Yili–Central Tianshan block), Siberian and Tarim plates were amalgamated at *ca.* 300 Ma (Bazhenov et al., 2003) and the clockwise rotation of the Tarim block is interpreted to have created the large scale intracontinental strike–slip movement between the Yili and Tarim blocks in Early Permian time (Wang et al., 2007a); (2) the Permian–Triassic intracontinental deformation has been documented to occur widespread in the Tianshan Orogen and adjacent regions (Yin and Nie, 1996; Shu et al., 1999; Laurent-Charvet et al., 2002; Laurent-Charvet et al., 2003; Charvet et al., 2007; Jong et al., 2009; Briggs et al., 2009; Yang et al., 2009); (3) the youngest ophiolite exposed in the Tianshan Orogen and adjacent regions is Early Carboniferous, with a SHRIMP U–Pb zircon age of 325 ± 7 Ma (Xu et al., 2005); (4) Permian continental molasses are regionally exposed in the North Tianshan Accretionary Complexes, along the northern margin and southern margin of the Yili block as well as the northern margin of Tarim block (Fig. 8); and (5) some "stitching" plutons occur in the North Tianshan suture zone (316 Ma; Han et al., 2010) (Fig. 1b), South Central Tianshan suture zone (276 Ma; Gao et al., 2009; 303 Ma, Seltmann et al., 2010) (Fig. 1b) and the northern margin of the Tarim block (296 Ma, Konopelko et al., 2007; 273 Ma, Wang et al., 2007b; 285 Ma, Long et al., 2008) (Fig. 1b).

Thus, the SP leucogranite dike, which crosscuts the HP–LT metamorphic belt, demonstrates that the closure of the 'South Tianshan Ocean' and the collision between the Yili and Tarim blocks must have taken place earlier than 285 Ma. In accordance with the evidence presented above, we can conclude that the amalgamation of the passive margin of the Tarim block with the active margin of the Siberia craton along the southwestern margin of the 'Altaids' lasted until the Late Carboniferous (from 320 Ma to 300 Ma), and not until the Early/Mid-Triassic as recently suggested (Zhang et al., 2007a, b; Xiao et al., 2009a).

7. Conclusion

1. The petrographical and geochemical data obtained for a leucocratic granite dike crosscutting the Tianshan HP–LT metamorphic belt indicate a strongly peraluminous bulk rock chemistry.
2. The zircon U–Pb age of 285 Ma obtained for SP leucogranites indicates that it intruded into the Tianshan HP–LT metamorphic belt during the early Permian. Thus, the HP–LT metamorphism must have occurred in the Tianshan Orogen before the onset of the Permian.

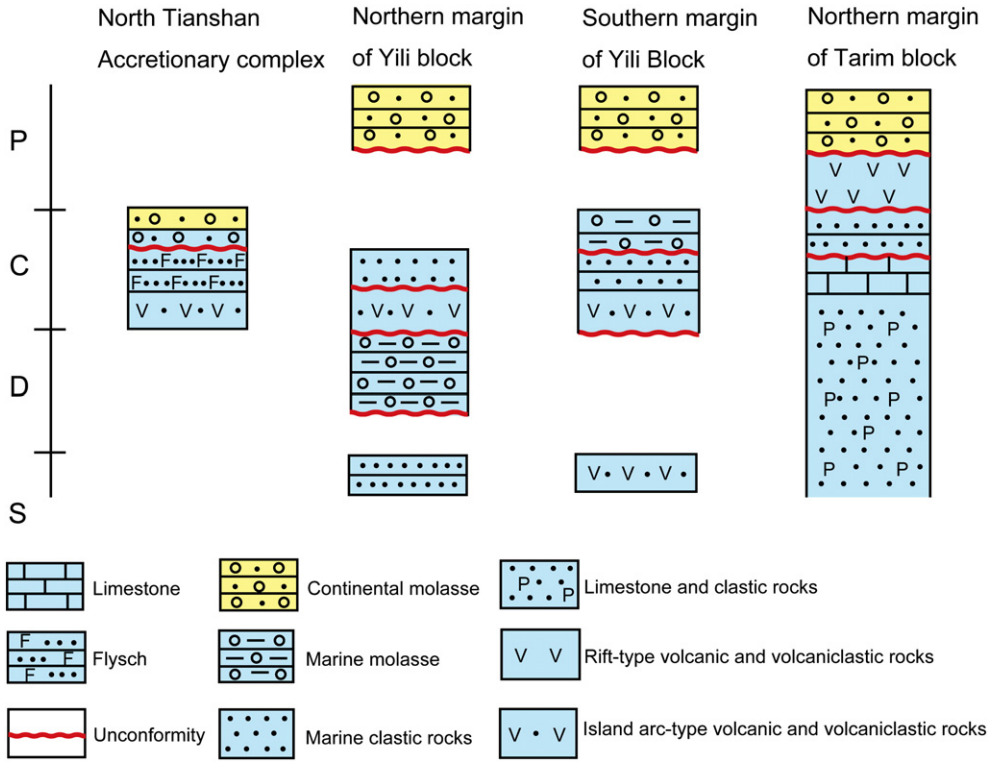

Fig. 8. Schematic stratigraphic diagram showing the Late Paleozoic strata of the North Tianshan Accretionary Complexes, the northern margin of the Yili block, the southern margin of the Yili block and the northern margin of the Tarim block (data after Wang et al., 1990, 1994; Gao et al., 1998).

3. The geochemical data further suggest that the SP leucogranite formed as a result of exhumation of overthickened crusts in a post-collisional setting, similar to the Himalaya 'high pressure' collision (e.g. Sylvester, 1998).
4. The collision between the Yili (–Central Tianshan) and Tarim blocks and the final amalgamation of the Southwestern Altaids must have been completed in Late Paleozoic and not Triassic times.

Acknowledgements

This research was supported by 'National Basic Research Program of China' (No. 2007CB411302), National Natural Science Foundation of China (41025008, 40672153, 4071062, and 40872057) and the Deutsche Forschungsgemeinschaft (KL 692/17-2). We are indebted to H. Li for conducting the XRF-analyses, X. D. Jin for the arrangement of the trace element analysis, X. H. Li and Q. L. Li for help conducting the Cameca IMS-1280 ion microprobe, C.F. Li and X.H. Li for the Nd isotope experiment. We thank G. M. Shu and U. Schüssler for their help with the microprobe measurements. We are indebted to three anonymous reviewers for their constructive comments and suggestions. Mian Liu is thanked for the editorial handling of the manuscript.

References

Ai, Y.L., Zhang, L.F., Li, X.P., Qu, J.F., 2005. The geochemistry characters of the HP–UHP eclogites and blueschist and its tectonic significance, Southwestern Tianshan, Xinjiang. Prog. Nat. Sci. 15, 1346–1356.
Allen, M.B., Windley, B.F., Zhang, C., 1992. Palaeozoic collisional tectonics and magmatism of the Chinese Tien Shan, central Asia. Tectonophysics 220, 89–115.
Barbarin, B., 1996. Genesis of the two main types of peraluminous granitoids. Geology 24, 295–298.
Barbarin, B., 1999. A review of the relationships between granitoid types, their origins and their geodynamic environments. Lithos 46, 605–626.
Bazhenov, M.L., Collins, A.Q., Degtyarev, K.E., Levashova, N.M., Mikolaichuk, A.V., Pavlov, V.E., Voo, R.V., 2003. Paleozoic northward drift of the North Tien Shan (Central Asia) as revealed by Ordovician and Carboniferous paleomagnetism. Tectonophysics 366, 113–141.
Beinlich, A., Klemd, R., John, T., Gao, J., 2010. Trace-element mobilization during Ca-metasomatism along a major fluid conduit: eclogitization of blueschist as a consequence of fluid–rock interaction. Geochim. Cosmochim. Acta 74, 1892–1922.
Bellieni, G., Cavazzini, G., Fioretti, A.M., Peccerillo, A., Zantedeschi, P., 1996. The Cima di Vila (Zinsnock) Intrusion, Eastern Alps: evidence for crustal melting, acid-mafic magma mingling and wall–rock fluid effects. Mineral. Petrol. 56, 125–146.
Biske, Y.S., Seltmann, R., 2010. Paleozoic Tian-Shan as a transitional region between the Rheic and Urals–Turkestan oceans. Gondwana Res. 17, 602–613.
Black, L.P., Kamo, S.L., Allen, C.M., Aleinikoff, J.N., Davis, D.W., Korsch, R.J., et al., 2003. TEMORA 1: a new zircon standard for Phanerozoic U–Pb geochronology. Chem. Geol. 200, 155–170.
Briggs, S.M., Yin, A., Manning, C.E., Chen, Z.L., Wang, X.F., 2009. Tectonic development of the southern Chinese Altai Range as determined by structural geology, thermobarometry, 40Ar/39Ar thermochronology, and Th/Pb ion-microprobe monazite geochronology. Geol. Soc. Am. Bull. 121, 1381–1393.
Brookfield, M.E., 2000. Geological development and Phanerozoic crustal accretion in the western segment of the southern Tien Shan (Kyrgyzstan, Uzbekistan and Tajikistan). Tectonophysics 328, 1–14.
Burtman, V.S., 2010. Tien Shan, Pamir, and Tibet: history and geodynamics of Phanerozoic oceanic basins. Geotectonics 44, 388–404.
Carroll, A.R., Graham, S.A., Hendrix, M.S., Ying, D., Zhou, D., 1995. Late Paleozoic tectonic amalgamation of northwestern China: sedimentary record of the north Tarim, northwestern Turpan and southern Junggar basins. Geol. Socity Am. Bull. 107, 571–594.
Charvet, J., Shu, L.S., Laurent-Charvet, S., 2007. Paleozoic structural and geodynamic evolution of eastern Tianshan (NW China): welding of the Tarim amd Junggar plates. Episodes 30, 162–186.
Chen, B., Jahn, B.M., 2004. Genesis of post-collisional granitoids and basement nature of the Junggar Terrane, NW China: Nd–Sr isotope and trace element evidence. J. Asia Earth Sci. 23, 691–703.
Chen, C.M., Lu, H.F., Jia, D., Cai, D.S., Wu, S., 1999. Closing history of the southern Tianshan oceanic basin, Western China: an oblique collsional orogeny. Tectonophysics 302, 23–40.
Coleman, R.G., 1989. Continental growth of northwest China. Tectonics 8, 621–635.
Dahlquist, J.A., Galindo, C., Pankhurst, R.J., Rapela, C.W., Alasino, P.H., Saavedra, J., Fanning, C.M., 2007. Magmatic evolution of the Penon Rosado granite: petrogenesis of garnet-bearing granitoids. Lithos 95, 177–207.
Gao, J., Klemd, R., 2001. Primary fluids entrapped at blueschist to eclogite transition: evidence from the Tianshan meta-subduction complex in northwestern China. Contrib. Mineralog. Petrol. 142, 1–14.
Gao, J., Klemd, R., 2003. Formation of HP–LT rocks and their tectonic implications in the western Tianshan Orogen, NW China: geochemical and age constraints. Lithos 66, 1–22.
Gao, J., He, G.Q., Li, M.S., Tang, Y.Q., Xiao, X.C., Zhou, M., Wang, J., 1995. The mineralogy, petrology, metamorphic PTDt trajectory and exhumation mechanism of blueschists, south Tianshan, northwestern China. Tectonophysics 250, 151–168.

Gao, J., Li, M.S., Xiao, X.C., Tang, Y., He, G.Q., 1998. Paleozoic tectonic evolution of the Tianshan orogen, northwestern China. Tectonophysics 287, 213–231.
Gao, J., Klemd, R., Zhang, L.F., Wang, Z.X., Xiao, X.C., 1999. P–T path of high pressure–low temperature rocks and tectonic implications in the western Tianshan Mountains (NW China). J. Metamorph. Geol. 17, 621–636.
Gao, J., Xiao, W.J., Li, J.Y., Han, B., Guo, .Z., Wang, J., 2002. 'Central-Asia type' orogenesis and metallogenesis in western China. IGCP 420 Project workshop (abstract), p. 39.
Gao, J., Long, L.L., Qian, Q., Huang, D.Z., Su, W., Klemd, R., 2006. South Tianshan: a late Paleozoic or a Triassic Orogen. Acta Petrologica Sin. 22 (5), 1049–1061 (in Chinese with English abstract).
Gao, J., Klemd, R., John, T., Xiong, X., 2007. Mobilisation of Ti–Nb–Ta during subduction: evidence from rutile-bearing segregations and veins hosted in eclogites, Tianshan, NW China. Geochim. Cosmochim. Acta 71, 4974–4996.
Gao, J., Long, L.L., Klemd, R., Qian, Q., Liu, D.Y., Xiong, X.M., Su, W., Liu, W., Wang, Y.T., Yang, F.Q., 2009. Tectonic evolution of the South Tianshan Orogen, NW China: geochemical and age constraints of granitoid rocks. Int. J. Earth Sci. 98, 1221–1238.
Gilotti, J.A., McClelland, W.C., 2007. Characteristics of, and a tectonic model for, ultrahigh-pressure metamorphism in the overriding plate of the Caledonian orogen. Int. Geol. Rev. 49, 777–797.
Glorie, S., Grave, J.D., Buslov, M.M., Elburg, M.A., Stockli, D.F., Gerdes, A., Van den Haute, P., 2010. Multi-method chronometric constraints on the evolution of the Northern Kyrgyz Tien Shan granitoids (Central Asian Orogenic Belt): from emplacement to exhumation. J. Asian Earth Sci. 38, 131–146.
Guo, S.S., Li, S.G., 2007. Petrological and geochemical constraints on the origin of leucogranites. Earth Sci. Front. 14 (6), 290–298 (in Chinese with English abstract).
Han, B.F., Wang, S.G., Jahn, B.M., Hong, D.W., Kagami, H., Sun, Y., 1997. Depleted-mantle source for the Ulungur River A-Type granites from North Xinjiang, Chian: geochemistry and Nd–Sr isotopic evidence, and implications for Phanerozoic crustal growth. Chem. Geol. 138, 135–159.
Han, B.F., He, G.Q., Wu, T.R., Li, H.M., 2004. Zircon U–Pb dating and geochemical features of early Paleozoic granites from Tianshan, Xinjiang: implications for tectonic evolution. Xinjiang Geol. 22 (1), 4–11 (in Chinese with English abstract).
Han, B.F., Guo, Z.J., Zhang, Z.C., Zhang, L., Chen, J.F., Song, B., 2010. Age, geochemistry, and tectonic implications of a late Paleozoic stitching pluton in the North Tian Shan suture zone, western. China Geol. Soc. Am. Bull. 122, 627–640.
Hegner, E., Klemd, R., Kröner, A., Corsini, M., Alexeiev, D.V., Iaccheri, L.M., Zack, T., Dulski, P., Xia, X., Windley, B.F., 2010. Mineralogy ages and P–T conditions of late Paleozoic high-pressure eclogite and provenance of mélange sediments in the South Tianshan Orogen of Kyrgyzstan. American Journal of Sciences (in press).
Heubeck, C., 2001. Assembly of central Asia during the middle and late Paleozoic. In: Hendrix, M.S., Davis, G.A. (Eds.), Paleozoic and Mesozoic tectonic evolution of central Asia: from continental assembly to intracontinental deformation: Geological Society of America Memoir, 194, pp. 1–22.
Hopson, C., Wen, J., Tilton, G., Tang, Y.Q., Zhu, B.Q., Zhao, M., 1989. Paleozoic plutonism in East Junggar, Bogdashan, and eastern Tianshan, NW China. EOS, Trans. American Geophysical Union 70, 1403–1404.
Inger, S., Harris, N., 1993. Geochemical constraints on leucogranite magmatism in the Langtang valley, Napal Himalaya. J. Petrol. 34, 345–368.
Jahn, B.M., 2004. Phanerozoic continental growth in Central Asia. J. Asian Earth Sci. 23, 599–603.
Jahn, B.M., Wu, F., Chen, B., 2000a. Granitoids of the Central Asian orogenic belt and continental growth in the Phanerozoic. Trans. R. Soc. Edinb. Earth Sci. 91, 181–193.
Jahn, B.M., Griffin, W.L., Windley, B.F., 2000b. Continental growth in the Phanerozoic: evidence from Central Asia. Tectonophysics 328 vii–x..
Jiang, C.Y., Mu, Y.M., Bai, K.Y., 1999. Chronology, petrology, geochemistry and tectonic environment in the southern Tianshan Mountain, western China. Acta Petrologica Sin. 15, 298–308 (in Chinese with English abstract).
John, T., Klemd, R., Gao, J., Garbe-Schonberg, C.D., 2008. Trace element mobilization in slabs due to non steady-state fluid–rock interaction: constraints from an eclogite-facies transport vein in blueschist (Tianshan, China). Lithos 103, 1–24.
Jong, K.D., Wang, B., Faure, M., Shu, L., Cluzel, D., Charvet, J., Ruffet, G., Chen, Y., 2009. New $^{40}Ar/^{39}Ar$ age constraints on the Late Paleozoic tectonic evolution of the western Tianshan (Xinjiang, northwestern China), with emphasis on Permian fluid ingress. Int. J. Earth Sci. 98, 1239–1258.
Klemd, R., 2003. Ultrahigh-pressure metamorphism in eclogites from the western Tianshan high-pressure belt (Xinjiang, western China)—comment. Am. Mineralog. 88, 1153–1156.
Klemd, R., Schröter, F.C., Will, T.M., Gao, J., 2002. PT-evolution of glaucophane-omphacite bearing HP–LT rocks in the western Tianshan orogen, NW China: new evidence for 'Alpine-type' tectonics. J. Metamorph. Geol. 20, 239–254.
Klemd, R., Bröcker, M., Hacker, B.R., Gao, J., Gans, P., Wemmer, K., 2005. New age constraints on the metamorphic evolution of the high-pressure/low-temperature belt in the western Tianshan Mountains, NW China. J. Geolgy 113, 157–168.
Konopelko, D., Biske, G., Seltmann, R., Eklun, O., Belyatsky, B., 2007. Hercynian post-collisional A-type granites of the Kokshaal Range, Southern Tien Shan. Lithos 97, 140–160.
Kröner, A., Windley, B.F., Badarch, G., Tomurtogoo, O., Hegner, E., Jahn, B.M., Gruschka, S., Khain, E.V., Demoux, A., Wingate, M.T.D., 2007. Accretionary growth and crust formation in the Central Asian Orogenic Belt and comparison with the Arabian–Nubian shield. In: Hatcher, R.D., Carlson, M.P., McBride, J.H., Martínez Catalán, J.R. (Eds.), 4-D Framework of Continental Crust: Geological Society of America Memoir, 200, pp. 181–209.
Kröner, A., Hegner, E., Lehmann, B., Heinhorst, J., Wingate, M.T.D., Liu, D.Y., Ermelov, P., 2008. Palaeozoic arc magmatism in the Central Asian Orogenic Belt of Kazakhstan: SHRIMP zircon ages and whole-rock Nd isotopic systematic. J. Asian Earth Sci. 32, 118–130.
Laurent-Charvet, S., Charvet, J., Shu, L.S., Ma, R.S., Lu, H.F., 2002. Paleozoic late collisional strike–slip deformations in Tianshan and Altay, Eastern Xinjinag, NW China. Terra Nova 14, 249–256.
Laurent-Charvet, S., Charvet, J., Monie', P., Shu, L.S., 2003. Late Paleozoic strike–slip shear zones in eastern central Asia (NW China): new structural and geochronological data. Tectonics 22, 1099–1101.
Le Fort, P., Cuney, M., Deniel, C., France-Lanord, C., Sheppard, S.M.F., Upreti, B.N., Vidal, P., 1987. Crustal generation of the Himalayan leucogranites. Tectonophysics 134, 39–57.
Lee, J., Whitehouse, M.J., 2007. Onset of mid-crustal extensional flow in southern Tibet: evidence from U/Pb zircon ages. Geology 35, 45–48.
Li, Q., Zhang, L.F., 2004. The P–T path and geological significance of low-pressure granulite-facies metamorphism in Muzhaert, southwest Tianshan. Acta Petrologica Sinica 20, 583–594.
Li, S., Wang, S., Chen, Y., Zhou, H., Zhang, Z., Liou, G., Qiou, J., 1994. Excess argon in phengite of eclogite: evidence from comparing dating of eclogite by Sm–Nd, Rb–Sr, and $^{40}Ar/^{39}Ar$ isotope method. Chem. Geol. 112, 343–350.
Li, J.Y., He, G.Q., Xu, X., Li, H.Q., Sun, G.H., Yang, T.N., Gao, L.M., Zhu, Z.X., 2006. Crustal tectonic framework of northern Tianshan and adjacent regions and its formation. Acta Geol. Sin. 80 (1), 149–168 (in Chinese with English abstract).
Li, X.P., Zhang, L.F., Wei, C.J., Ai, Y., Chen, J., 2007. Petrology of rodingite derived from eclogite in western Tianshan, China. J. Metamorph. Geol. 25, 363–382.
Li, X.G., Liu, S.W., Wang, Z.Q., Han, B.F., Shu, G.M., Wang, T., 2008. Electron microprobe monazite geochronological constraints on the Late Palaeozoic tectonothermal evolution in the Chinese Tianshan. J. Geol. Soc. Lond. 165, 511–522.
Li, X.H., Liu, Y., Li, Q.L., Guo, C.H., Chamberlain, K.R., 2009. Precise determination of Phanerozoic zircon Pb/Pb age by multi-collector SIMS without external standardization. Geochem. Geophys. Geosyst. 10 (4), 1–21.
Li, Q.L., Lin, W., Su, W., Li, X.H., Shi, Y.H., Liu, Y., Tang, G.Q., 2010a. SIMS U–Pb rutile age of low-temperature eclogites from southwestern Chinese Tianshan, NW China. Lithos. doi:10.1016/j.lithos.2010.11.007.
Li, X.P., Zhang, L.F., Wilde, S.A., Song, B., Liu, X.M., 2010b. Zircons from rodingite in the Western Tianshan serpentinite complex: mineral chemistry and U–Pb ages define nature and timing of rodingitization. Lithos 118, 17–34.
Liao Ning Institute of Geological Survey 2005. Geological map of the Akesu region, scale 1:50,000, Explanation. Urimqi, pp 1–175 (in Chinese).
Liégeois, J.P., 1998. Preface — some words on the post-collisional magmatism. Lithos 45 xv–xvii.
Lin, W., Enami, M., 2006. Prograde pressure–temperature path of jadeite-bearing eclogites and associated high-pressure/low-temperature rocks from western Tianshan, northwest China. The Island Arc 15, 483–502.
Lin, W., Faure, M., Shi, Y.H., Wang, Q.C., Li, Z., 2009. Palaeozoic tectonics of the south-western Chinese Tianshan: new insights from a structural study of the high-pressure/low-temperature metamorphic belt. Int. J. Earth Sci. 98, 1259–1274.
Liu, C.X., Xu, B.L., Zhou, T.R., 2004. Petrochemistry and tectonic significance of Hercynian alkaline rocks along the northern margin of the Tarim platform and its adjacent area. Xinjiang Geol. 22, 43–49 (in Chinese with English abstract).
Long, L.L., Gao, J., Qian, Q., Xiong, X.M., Wang, J.B., Wang, Y.W., Wang, L.J., 2008. Geochemistry and SHRIMP zircon U–Pb age of post-collisional granites in the southwest Tianshan Orogenic Belt of China: examples from the Heiyingshan and Laohutai plutons. Acta Geol. Sin. 82, 415–424.
Lü, Z., Zhang, L.F., Du, J., Bucher, K., 2008. Coesite inclusions in garnet from eclogitic rocks in western Tianshan, northwest China: convincing proof of UHP metamorphism. Am. Mineralog. 93, 1845–1850.
Lü, Z., Zhang, L.F., Du, J., Bucher, K., 2009. Petrology of coesite-bearing eclogite from Habutengsu Valley, western Tianshan, NW China and its tectonometamorphic implication. J. Metamorph. Geol. 27, 773–787.
Ludwig, K.R., 2001. Users Manual for Isoplot/Ex rev. 2.49. Berkeley Geochronology Centre Special Publication. No. 1a, p. 56.
Maniar, P.D., Piccoli, P.M., 1989. Tectonic discrimination of granitoids. Geol. Soc. Am. Bull. 101, 635–643.
Middlemost, E.A.K., 1994. Naming materials in the magma/igneous rocks system. Earth Sci. Rev. 37, 215–224.
Nabelek, P.I., Bartlett, C.D., 1998. Petrologic and geochemical links between the post-collisional Proterozoic Harney Peak leucogranite, South Dakota, USA, and its source rocks. Lithos 45, 71–85.
Pearce, J.A., Harris, N.B.W., Tindle, A.G., 1984. Trace element discrimination diagrams for the tectonic interpretation of granitic rocks. J. Petrol. 25, 956–983.
Qian, Q., Gao, J., Klemd, R., He, G., Xiong, X.M., Long, L.L., et al., 2009. Early Paleozoic tectonic evolution of the Chinese South Tianshan Orogen: constraints from SHRIMP zircon U–Pb geochronology and geochemistry of basaltic and dioritic rocks from Xiate, NW China. Int. J. Earth Sci. 98, 551–569.
Ren, R., Han, B.F., Ji, J.Q., Zhang, L., Xu, Z., Su, L., 2010. U–Pb age spectra of detrital zircons from the Tekes River, Xinjiang, China, and implications for tectonomagmatic evolution of the South Tian Shan Orogen. Gondwana Res. doi:10.1016/j.gr.2010.07.005.
Rubatto, D., Hermann, J., 2003. Zircon formation during fluid circulation in eclogites (Monviso, Western Alps): implications for Zr and Hf budget in subduction zones. Geochim. Cosmochim. Acta 67, 2173–2187.
Schärer, U., Xu, R.H., Allegre, C.J., 1986. U–Th–Pb systematic and ages of Himalayan leucogranites, south Tibet. Earth Planet. Sci. Lett. 77, 35–48.
Schmädicke, E., Mezger, K., Cosca, M.A., Okrusch, M., 1995. Variscan Sm–Nd and Ar–Ar ages of eclogite facies rocks from the Erzgebirge, Bohemian Massif. J. Metamorph. Geol. 13, 537–552.
Searle, M.P., Parrish, R.R., Hodges, K.V., Hurford, A., Ayres, M.W., Whitehouse, M.J., 1997. Shisha Pangma leucogranite, south Tibetan Himalaya: field relations, geochemistry, age, origin, and emplacement. J. Geol. 105, 295–317.

Seltmann, R., Konopelko, D., Biske, G., Divaev, F., Serge, S., 2010. Hercynian post-collisional magmatism in the context of Paleozoic magmatic evolution of the Tien Shan orogenic belt. J. Asian Earth Sci. doi:10.1016/j.jseaes.2010.08.016.

Sengör, A.M.C., Natal'In, B.A., Burtman, V.S., 1993. Evolution of the Altaid tectonic collage and Paleozoic crustal growth in Eurasia. Nature 364, 299–307.

Shi, Y.R., Liu, D.Y., Zhang, Q., Jian, P., Zhang, F.Q., Miao, L.C., 2007. SHRIMP zircon U–Pb dating of the Gangou granitoids, Central Tianshan Mountains, Northwest China and tectonic significances. Chinese Science Bulletin 52, 1507–1516.

Shu, L.S., Charvet, J., Guo, L.Z., Lu, H.F., 1999. A large-scale Paleozoic dextral ductile strike–slip zone: the Aqqikkudug–Weiya zone along the northern margin of the Central Tianshan belt, Xinjiang, NW China. Acta Geol. Sin. 73 (2), 148–162.

Simonov, V.A., Sakiev, K.S., Volkova, N.I., Stupakov, S.I., Travin, A.V., 2008. Conditions of formation of the Atbashi Ridge eclogites (South Tien Shan). Russ. Geol. Geophys. 49, 803–815.

Solomovich, L.I., 2007. Postcollisional magmatism in the South Tien Shan Variscan orogenic belt, Kyrgyztan: evidence for high-temperature and high-pressure collision. J. Asian Earth Sci. 30, 142–153.

Solomovich, L.I., Trifonov, B.A., 2002. Postcollisional granites in the South Tien Shan Variscan collisional belt, Kyrgyztan. J. Asian Earth Sci. 21, 7–21.

Stacey, J.S., Kramers, J.D., 1975. Approximation of terrestrial lead isotope evolution by a two-stage model. Earth Planet. Sci. Lett. 26, 207–221.

Su, W., Gao, J., Klemd, R., Li, J.L., Zhang, X., Li, X.H., Chen, N.S., Zhang, L., 2010. U–Pb zircon geochronology of Tianshan eclogites in NW China: implication for the collision between the Yili and Tarim blocks of the southwestern Altaids. Eur. J. Mineralog. 22, 473–478.

Sun, S.S., McDonough, W.F., 1989. Chemical and isotopic systematics of oceanic basalts: implications for mantle composition and processes. In: Saunders, A.D., Norry, M.J. (Eds.), Magmatism in the Ocean Basin. Geol. Soc. Spec. Pub. 42, 313–345.

Sylvester, P.J., 1998. Post-collisional strongly peraluminous granites. Lithos 45, 29–44.

Tagiri, M., Yano, T., Bakirov, A., Nakajima, T., Uchiumi, S., 1995. Mineral parageneses and metamorphic P–T paths of ultrahigh-pressure eclogites from Kyrgyzstan Tien-Shan. Island Arc 4, 280–292.

Taylor, S.R., McLennan, S.M., 1985. The Continental Crust: Its Composition and Evolution. Oxford, Blackwell. pp. 312.

Van der Straaten, F., Schenk, V., John, T., Gao, J., 2008. Blueschist-facies rehydration of eclogites (Tian Shan, NW-China): implications for fluid–rock interaction in the subduction channel. Chem. Geol. 255, 195–219.

Volkova, N.I., Budanov, V.I., 1999. Geochemical discrimination of metabasalt rocks of the Fan-Karategin transitional blueschist/greenschist belt, South Tianshan, Tajikistan: seamount volcanism and accretionary tectonics. Lithos 47, 201–216.

Von Blanckenburg, F., 1992. Combined high-precision chronometry and geochemical tracing using accessory minerals: applied to the Central-Alpine Bergell intrusion (Central Europe). Chem. Geol. 100, 19–40.

Wang, Z.X., Wu, J.Y., Liu, C.H., Lu, X.C., Zhang, J.G., 1990. . 217 pp Polycyclic Tectonic Evolution and Metallogeny of the Tianshan Mountains. Science Press, Beijing (in Chinese with English abstract).

Wang, B.Y., Lang, Z.J., Li, X.D., 1994. Study on the Geological Sections Across the Western Segment of Tianshan Mountains. Science Press, China. Beijing, pp. 1–202 (in Chinese).

Wang, B., Chen, Y., Zhan, S., Shu, L.S., Faure, M., Cluzel, D., Charvet, J., Laurent-Charvet, S., 2007a. Primary Carboniferous and Permian paleomagnetic results from the Yili Block (NW China) and their implications on the geodynamic evolution of Chinese Tianshan Belt. Earth Planet. Sci. Lett. 263, 288–308.

Wang, C., Liu, L., Luo, J.H., Che, Z.C., Teng, Z.H., Cao, X.D., Zhang, J.Y., 2007b. Late Paleozoic post-collisional magmatism in the Southwestern Tianshan orogenic belt: an example from the Baleigong pluton in the Kokshal region. Acta Petrologica Sin. 23 (8), 1830–1840 (in Chinese with English abstract).

Wang, B., Faure, M., Shu, L.S., Jong, K.D., Charvet, J., Cluzel, D., Jahn, B.M., Chen, Y., Ruffet, G., 2010. Structural and geochronological study of high-pressure metamorphic rocks in the Kekesu Section (Northwestern China): implications for the Late Paleozoic tectonics of the Southern Tianshan. J. Geol. 118, 59–77.

Wang, B., Shu, L.S., Faure, M., Jahn, B.M., Cluzel, D., Charvet, J., Chung, S.L., Meffre, S., 2011. Paleozoic tectonics of the southern Chinese Tianshan: insights from structural, chronological and geochemical studies of the Heiyingshan ophiolitic mélange (NW China). Tectonophysics. doi:10.1016/j.tecto.2010.11.004.

Wei, C.J., Powell, R., Zhang, L.F., 2003. Eclogites from the south Tienshan, NW China: petrological characteristic and calculated mineral equilibria in the Na_2O–CaO–FeO–MgO–Al_2O_3–SiO_2–H_2O system. J. Metamorph. Geol. 21, 163–179.

Wei, C.J., Wang, W., Clarke, G.L., Zhang, L.F., Song, S.G., 2009. Metamorphism of high/ultrahigh-pressure pelitic–felsic schist in the South Tianshan Orogen, NWChina: phase equilibria and P–T path. J. Petrol. 50, 1973–1991.

White, W.M., 2007. Geochemistry. John-Hopkins University Press, pp. 313–358.

Wiedenbeck, M., Alle, P., Corfu, F., Griffin, W.L., Meier, M., Oberli, F., Vonquadt, A., Roddick, J.C., Speigel, W., 1995. Three natural zircon standards for U–Th–Pb, Lu–Hf, trace-element and REE analyses. Geostand. Newsl. 19, 1–23.

Windley, B.F., 1995. The Evolving Continent, 3 rd edition. John Wiley & Sons, Chichester. pp. 1–526.

Windley, B.F., Allen, M.B., Zhang, C., Zhao, Z., Wang, Q., 1990. Paleozoic accretion and Cenozoic redeformation of the Chinese Tien Shan range, central Asia. Geology 18, 128–131.

Windley, B.F., Alexeiev, D., Xiao, W., Kröner, A., Badarch, G., 2007. Tectonic models for accretion of the Central Asian Orogenic Belt. J. Geol. Soc. Lond. 164, 31–47.

Wu, F.Y., Huang, B.C., Ye, K., Fang, A.M., 2008. Collapsed Himalayan–Tibetan orogen and rising Tibetan Plateau. Acta Petrologica Sin. 24 (1), 1–30 (in Chinese with English abstract).

Xia, L.Q., Xu, X.Y., Xia, Z.C., Li, X.M., Ma, Z.P., Wang, L.S., 2004. Petrogenesis of Carboniferous rift-related volcanic rocks in the Tianshan, northwestern China. Geol. Soc. Am. Bull. 116, 419–433.

Xiao, X.C., Tang, Y.Q., Feng, Y.M., Zhu, B.Q., Li, J.Y., Zhao, M., 1992. Tectonic Evolution of Northern Xinjiang and Its Adjacent Regions. Geological Publishing House, Beijing, pp. 1–169 (in Chinese with English abstract).

Xiao, W.J., Zhang, L.C., Qin, K.Z., Sun, S., Li, J.L., 2004. Paleozoic accretionary and collisional tectonics of the eastern Tianshan (CHINA): implications for the continental growth of Central Asia. Am. J. Sci. 304, 370–395.

Xiao, W.J., Han, C.M., Yuan, C., Chen, H.L., Sun, M., Lin, S.F., Li, Z.L., Mao, Q.G., Zhang, J.E., Sun, S., Li, J.L., 2006. The unique Carboniferous–early Permian tectonic–metallogenic framework of Northern Xinjiang (NW China): constraints for the tectonics of the southern Paleoasian Domain. Acta Petrologica Sin. 22 (5), 1062–1076 (in Chinese with English abstract).

Xiao, W.J., Windley, B.F., Huang, B.C., Han, C.M., Yuan, C., Chen, H.L., Sun, M., Sun, S., Li, J.L., 2009a. End-Permian to mid-Triassic termination of the accretionary processes of the southern Altaids: implications for the geodynamic evolution, Phanerozoic continental growth, and metallogeny of Central Asia. Int. J. Earth Sci. 98, 1189–1217.

Xiao, W.J., Kröner, A., Windley, B.F., 2009b. Geodynamic evolution of Central Asia in the Paleozoic and Mesozoic. Int. J. Earth Sci. 98, 1185–1188.

Xu, X.Y., Ma, Z.P., Xia, L.Q., Wang, Y.B., Li, X.M., Xia, Z.C., Wang, L.S., 2005. SHRIMP dating of plagio granites from Bayingou ophiolite in the northern Tianshan Mountains. Geol. Rev. 22, 523–527 (in Chinese with English abstract).

Yakubchuk, A., 2004. Architecture and mineral deposit settings of the Altaid orogenic collage: a revised model. J. Asian Earth Sci. 23, 761–779.

Yang, S.H., Zhou, M.F., 2009. Geochemistry of the ~430 Ma Jingbulake mafic–ultramafic intrusion in Western Xinjiang, NW China: implications for subduction related magmatism in the South Tianshan orogenic belt. Lithos 113, 259–273.

Yang, T.N., Li, J.Y., Wang, Y., Dang, Y.X., 2009. Late Early Permian (266 Ma) N–S compressional deformation of the Turfan basin, NW China: the cause of the change in basin pattern. Int. J. Earth Sci. 98, 1311–1324.

Yin, A., Harrison, T.M., 2000. Geologic evolution of the Himalayan–Tibetan orogen. Annu. Rev. Earth Planet. Sci. 28, 211–280.

Yin, A., Nie, S., 1996. A Phanerozoic palinspastic reconstruction of China and its neighboring regions. In: Yin, A., Harrison, T.M. (Eds.), The Tectonic Evolution of Asia. Cambridge University Press, Cambridge, pp. 442–485.

Yin, A., Nie, S., Craig, P., Harrison, T.M., Ryerson, F.J., Qian, X.L., Yang, G., 1998. Late Cenozoic tectonic evolution of the southern Chinese Tian Shan. Tectonics 17, 1–27.

Zhang, L., Ellis, D.J., Arculus, R.J., Jiang, W., Wei, C., 2003a. Forbidden zone subduction of sediments to 150 km depth — the reaction of dolomite to magnesite + aragonite in the UHPM metapelites from western Tianshan, China. J. Metamorph. Geol. 21, 523–529.

Zhang, L.F., Ellis, D.J., Williams, S., Jiang, W., 2003b. Ultrahigh pressure metamorphism in eclogites from the Western Tianshan, China — reply. Am. Mineralog. 88, 1157–1160.

Zhang, H.F., Harris, N., Parrish, R., Kelley, S., Zhang, L., Rogers, N., Argles, T., King, J., 2004. Causes and consequences of protracted melting of the mid-crust exposed in the North Himalayan antiform. Earth Planet. Sci. Lett. 228, 195–212.

Zhang, L.F., Ai, Y.L., Li, X.P., Rubatto, D., Song, B., Williams, S., Song, S.G., Ellis, D., Liou, J.G., 2007a. Triassic collision of western Tianshan orogenic belt, China: evidence from SHRIMP U–Pb dating of zircon from HP/UHP eclogitic rocks. Lithos 96, 266–280.

Zhang, L.F., Ai, Y.L., Song, S.G., Liou, J., Wei, C.J., 2007b. A brief review of UHP meta-ophiolitic rocks, Southwestern Tianshan, Western China. Int. Geol. Rev. 49, 811–823.

Zhang, L.F., Du, J., Lu, Z., Song, S., Wei, C., 2009. The Timing of UHP–HP Eclogitic Rocks in Western Tianshan, NW China: The New SIMS U–Pb Zircon Dating, Lu/Hf and Sm/Nd Isochron Ages: Abstract Volume, 8th International Eclogite Conference. Xining, China. p. 177.

Zhao, Z.H., Bai, Z.H., Xiong, X.L., Mei, H.J., Wang, Y.X., 2000. Geochemistry of alkali-rich igneous rocks of Northern Xinjiang and its implications for geodynamics. Acta Geol. Sin. 74 (2), 321–328.

Zhao, Z.H., Xiong, X.L., Wang, Q., Wyman, D.A., Bao, Z.W., Bai, Z.H., Qiao, Y.L., 2008. Underplating-related adakites in Xinjiang Tianshan, China. Lithos 102, 374–391.

Zhou, D., Graham, S.A., Chang, E.Z., Wang, B., Hacker, B., 2001. Paleozoic tectonic amalgamation of the Chinese Tian Shan: evidence from a transect along the Dushanzi–Kuqa highway. In: Hendrix, M.S., Davis, G.A. (Eds.), Paleozoic and Mesozoic tectonic evolution of central Asia: from continental assembly to intracontinental deformation. Geological Society of American Memoir, 194, pp. 23–46.

Zhou, M.F., Lesher, C.M., Yang, Z.X., Li, J.W., Sun, M., 2004. Geochemistry and petrogenesis of 270 Ma Ni–Cu–(PGE) sulfide-bearing mafic intrusions in the Huangshan district, Eastern Xinjiang, Northwestern China: implications for the tectonic evolution of the Central Asian orogenic belt. Chem. Geol. 209, 233–257.

Zhu, Y.F., Zhang, L.F., Gu, L.B., Guo, X., Zhou, J., 2005. SHRIMP geochronologyand element geochemistry of Carboniferous volcanic rocks in the western Tianshan area. Chin. Sci. Bull. 50, 2004–2014.

Zhu, Z.X., Li, J.Y., Dong, L.H., Wang, K.Z., Liu, G.Z., Li, Y.P., Liu, Z.T., 2008. Age determination and geological significance of Devonian granitic intrusion in Serikeyayilake region, northern margin of Tarim basin. Acta Petrologica Sin. 24 (5), 971–976 (in Chinese with English abstract).

Zonenshain, L.P., Kuzmin, M.I., Natapov, L.M., 1990. Geology of the USSR: a plate-TECTONIC SYNTHESIS. In: Page, B.M. (Editor), American Geophysics Union, Geodynamics. Series 21, 1–242.